

MHD Waves and Instabilities

Chris Nelson, ESA/ESTEC

STFC Summer School, Sheffield

02/09/24



2007–2011

MMath

University of Sheffield

2011–2015

PhD

*University of Sheffield &
Armagh Observatory*

2015–2022

Various Post-Docs

*University of Sheffield &
Queen's University Belfast*

2022–Present

Research Fellow

*European Space Research and Technology Centre,
European Space Agency*

Who am I?

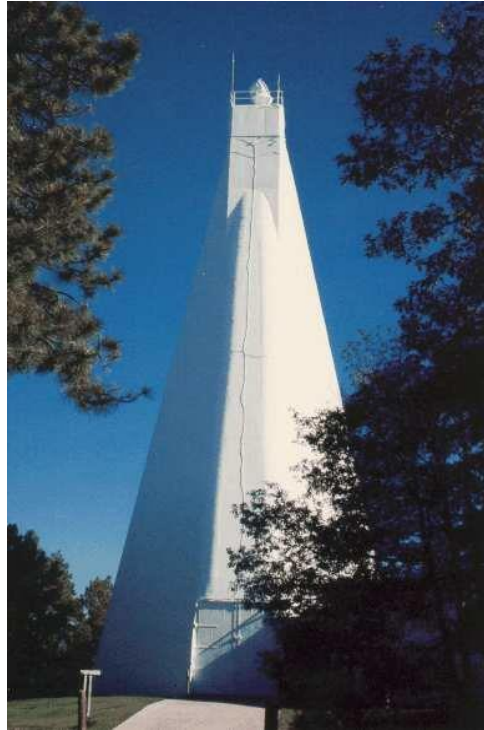


Who am I?

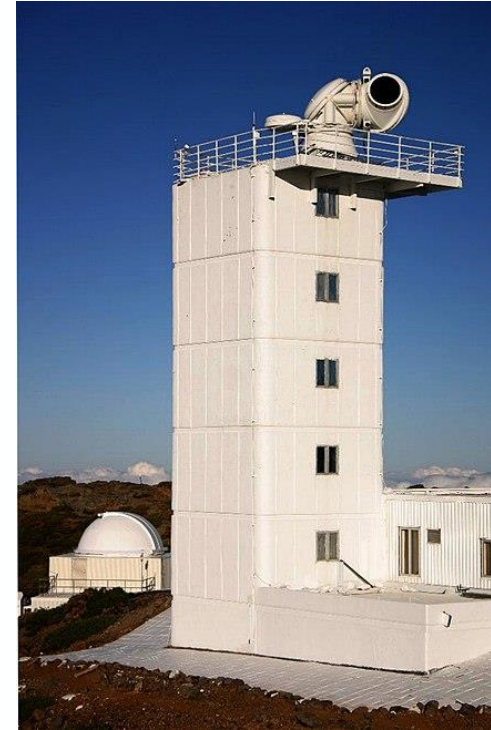
Began my career by gaining experience in experimental observational solar physics by spending (a lot of) time at three different ground-based solar telescopes.

Many of these opportunities came about through funding from the **SOLARNET** project.

I am also a member of the Science Advisory Group for the next generation **European Solar Telescope**.



Dunn Solar Telescope



Swedish Solar Telescope



GREGOR

Who am I?

More recently, I have also become involved in space-borne missions such as NASA's *Interface Region Imaging Spectrograph* (IRIS) as a **Science Planner** and the European Space Agency's *Solar Orbiter* as a **Solar Orbiter Observing Plan (SOOP) Coordinator**.



Interface Region Imaging Spectrograph

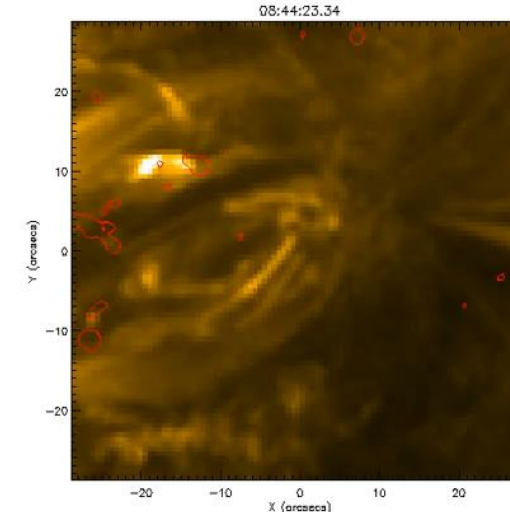
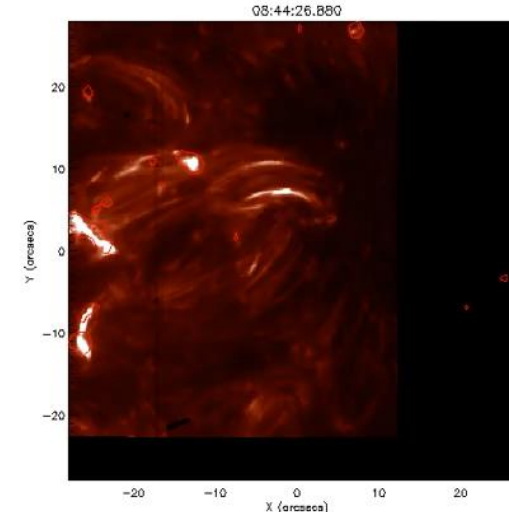
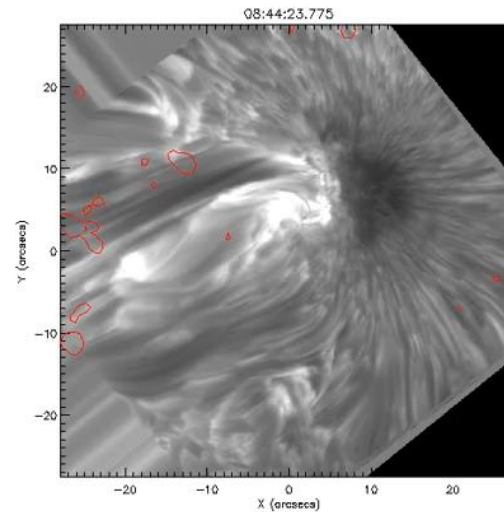
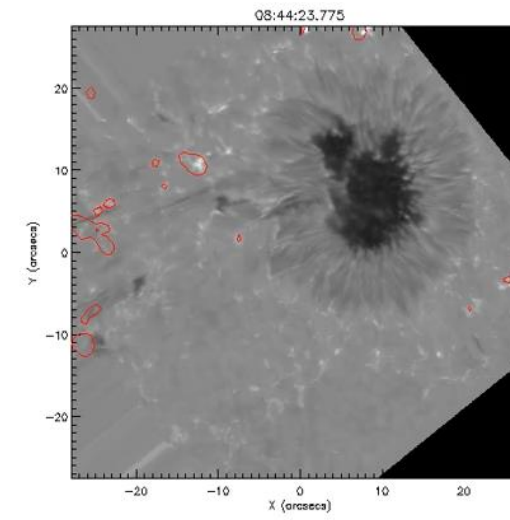
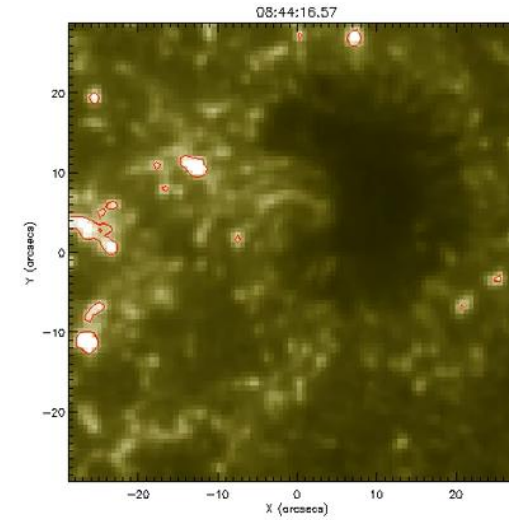
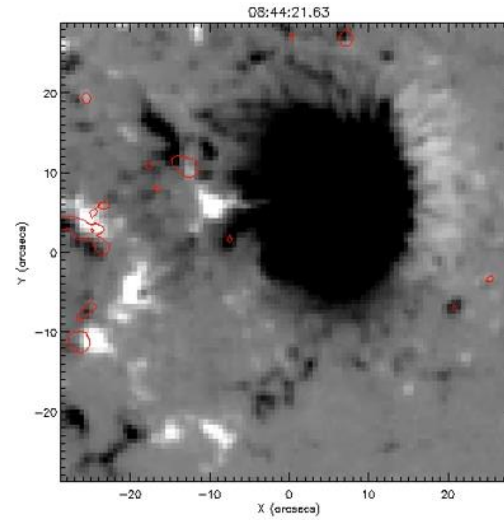


Solar Orbiter

Who am I?

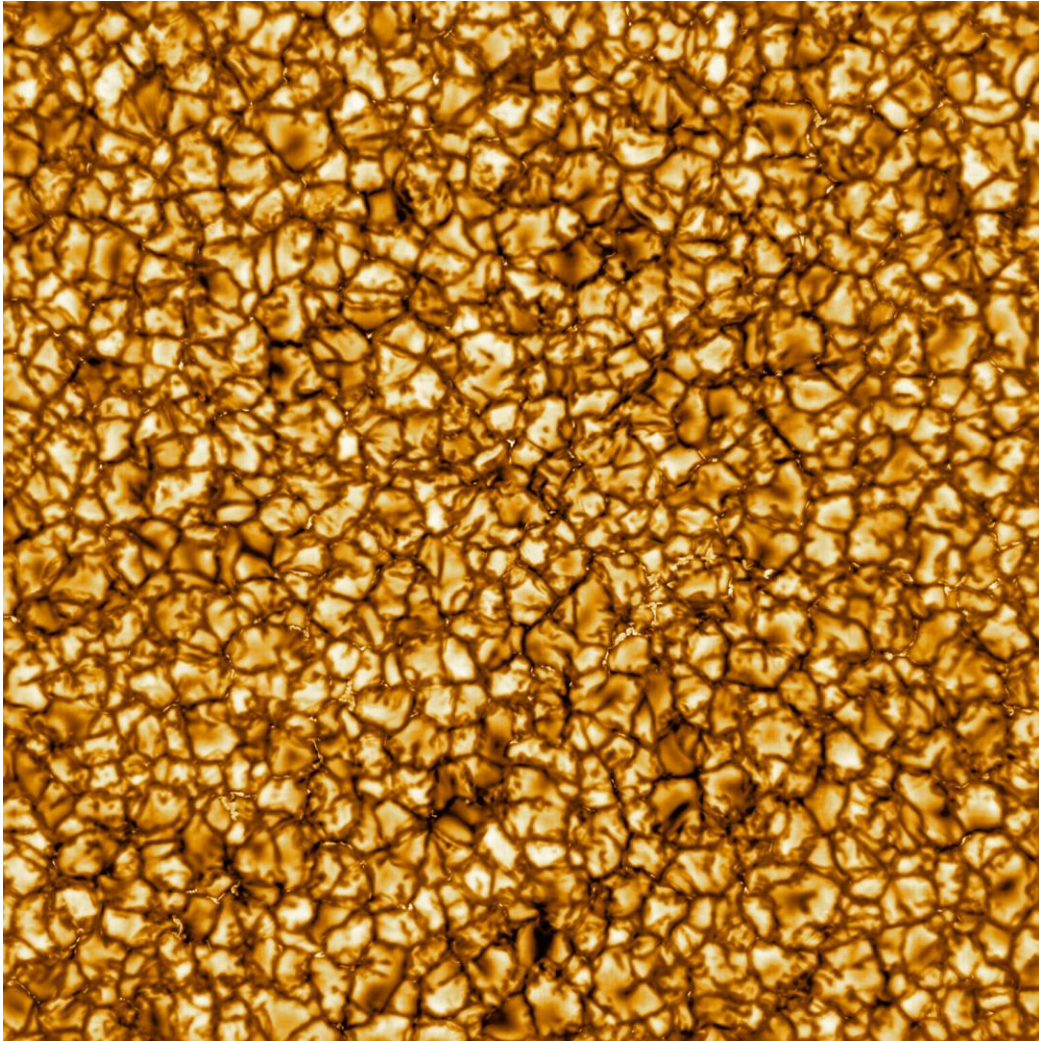
I am interested in how energy is transported **from the lower layers** of the solar atmosphere **into the upper layers** of the solar atmosphere, and how it is dissipated when it gets there.

For this, we need a combination of ground-based instruments (which are very good at observing the lower solar atmosphere) and space-borne instruments (which are very good at observing the upper solar atmosphere).



1. Introduction to magnetic waveguides
2. Introduction to magnetohydrodynamic (MHD) waves
3. Introduction to MHD instabilities

Introduction to magnetic waveguides



The photosphere is the lowest region of the Sun that we can directly observe.

Temperature ~ 6000 K

Density $\sim 10^{23}$ m⁻³

Height $\sim <600$ km

In the quiet-Sun, the photosphere is dominated by granular motions and magnetic bright points. In Active Regions, it is dominated by large-scale sunspots and pores.

Credit: NSO/NSF/AURA

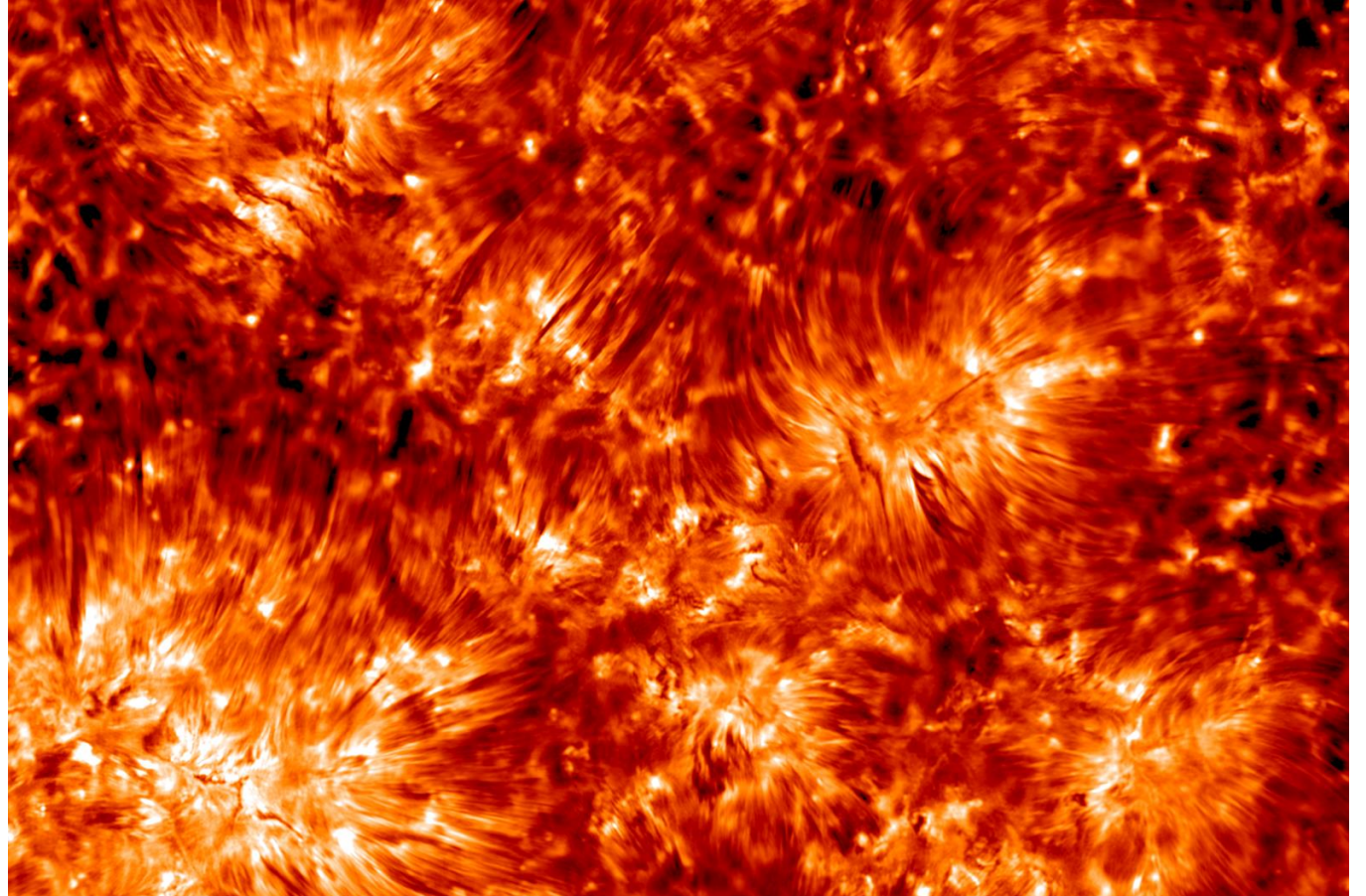
Above the photosphere, lies the complex and dynamic chromosphere.

Temperature $\sim < 50000$ K

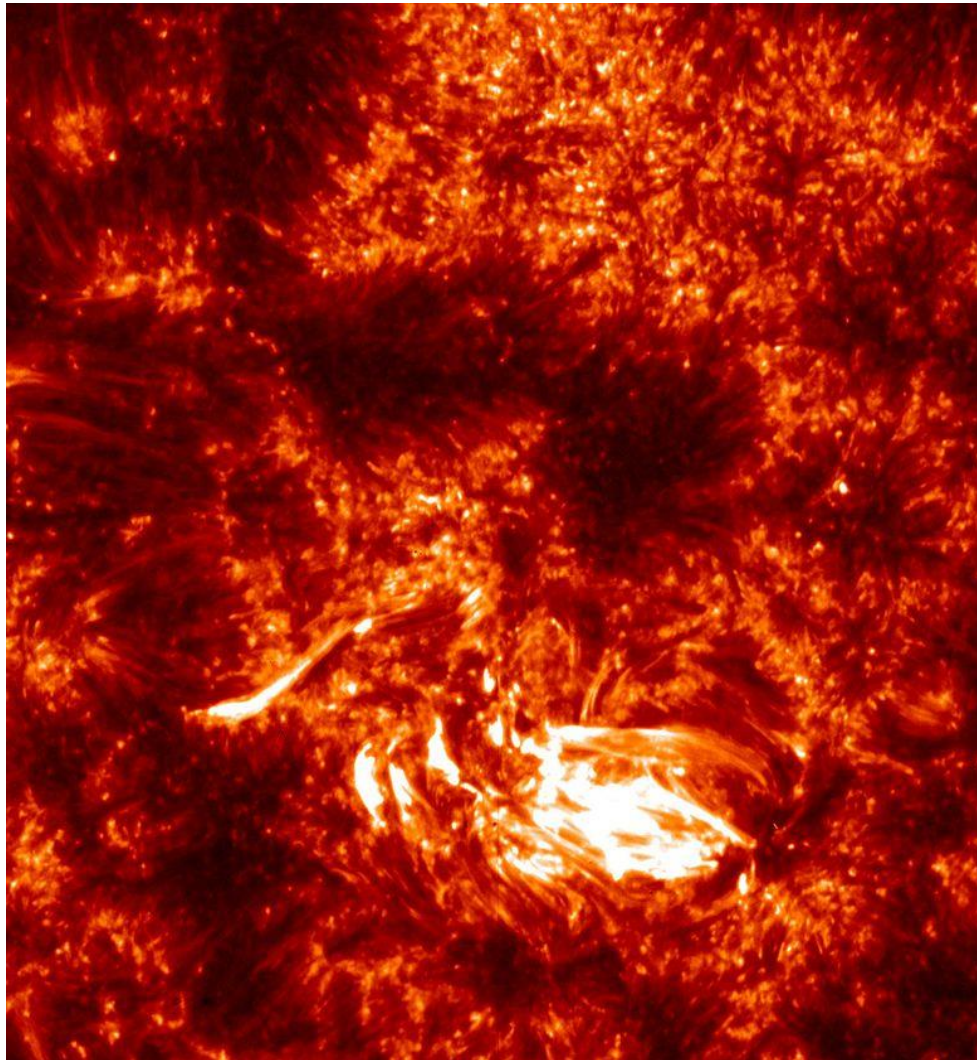
Density $\sim 10^{19} \text{ m}^{-3}$

Height $\sim 600\text{-}2000$ km

The chromosphere is dominated by long, thin fibril structures which seem almost horizontal in nature.



Credit: SST/CHROMIS



The transition region is a thin region above the chromosphere where the temperature rises extremely quickly.

Temperature $\sim 50000-100000$ K

Density $\sim 10^{16} \text{ m}^{-3}$

Height ~ 2000 km

Host to a range of features and physical processes which all combine to make this region extremely complicated to model.

Credit: IRIS/LMSAL/NASA

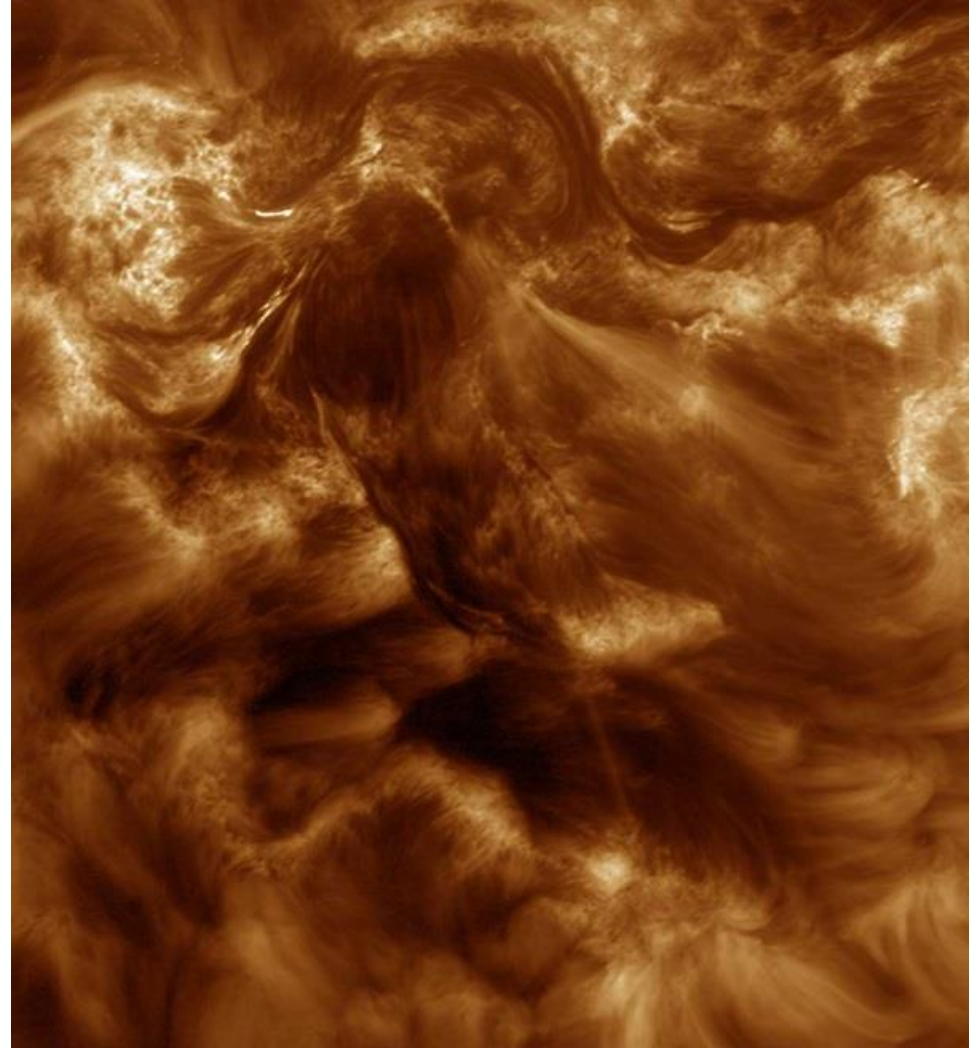
The vast region stretching out into space above the transition region.

Temperature $\sim 100000 < K$

Density $\sim < 10^{15} \text{ m}^{-3}$

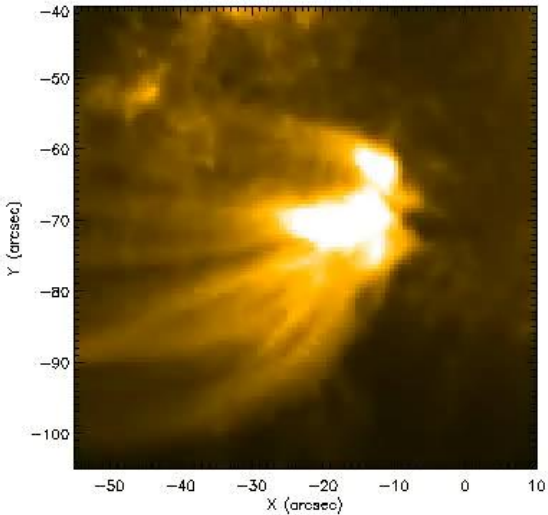
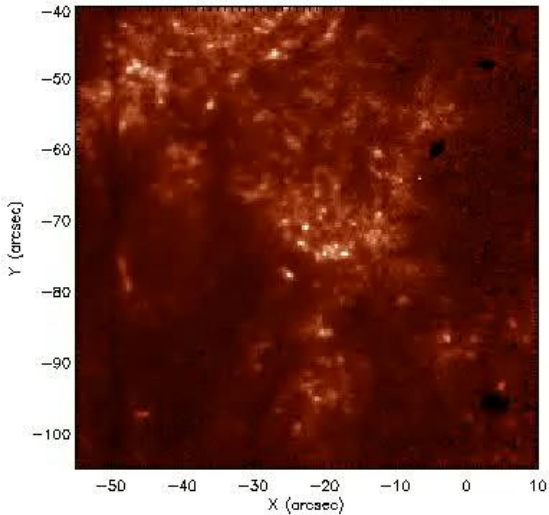
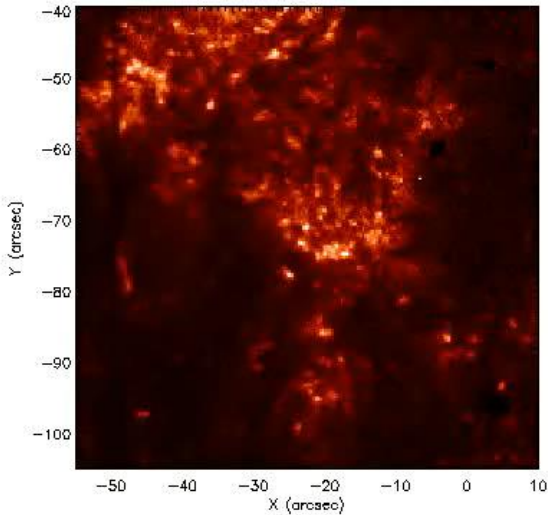
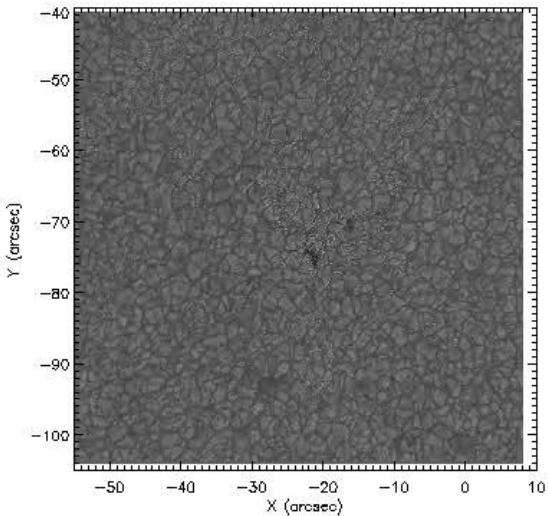
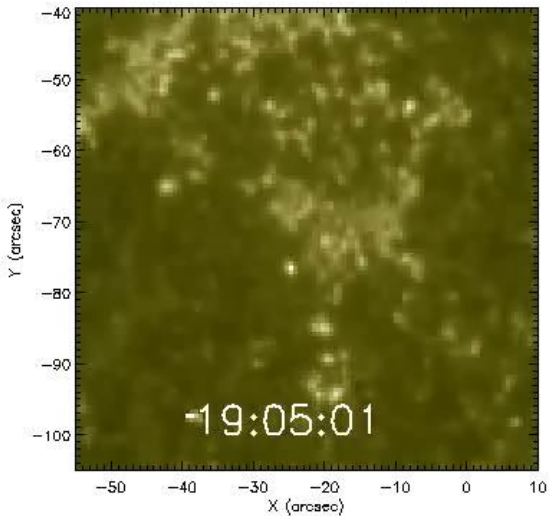
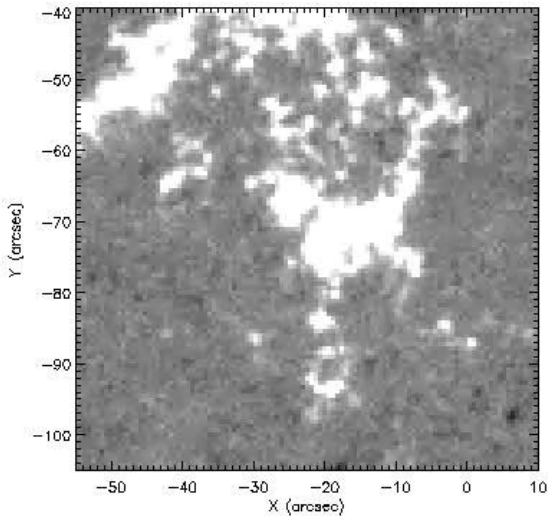
Height $\sim 2000 < \text{km}$

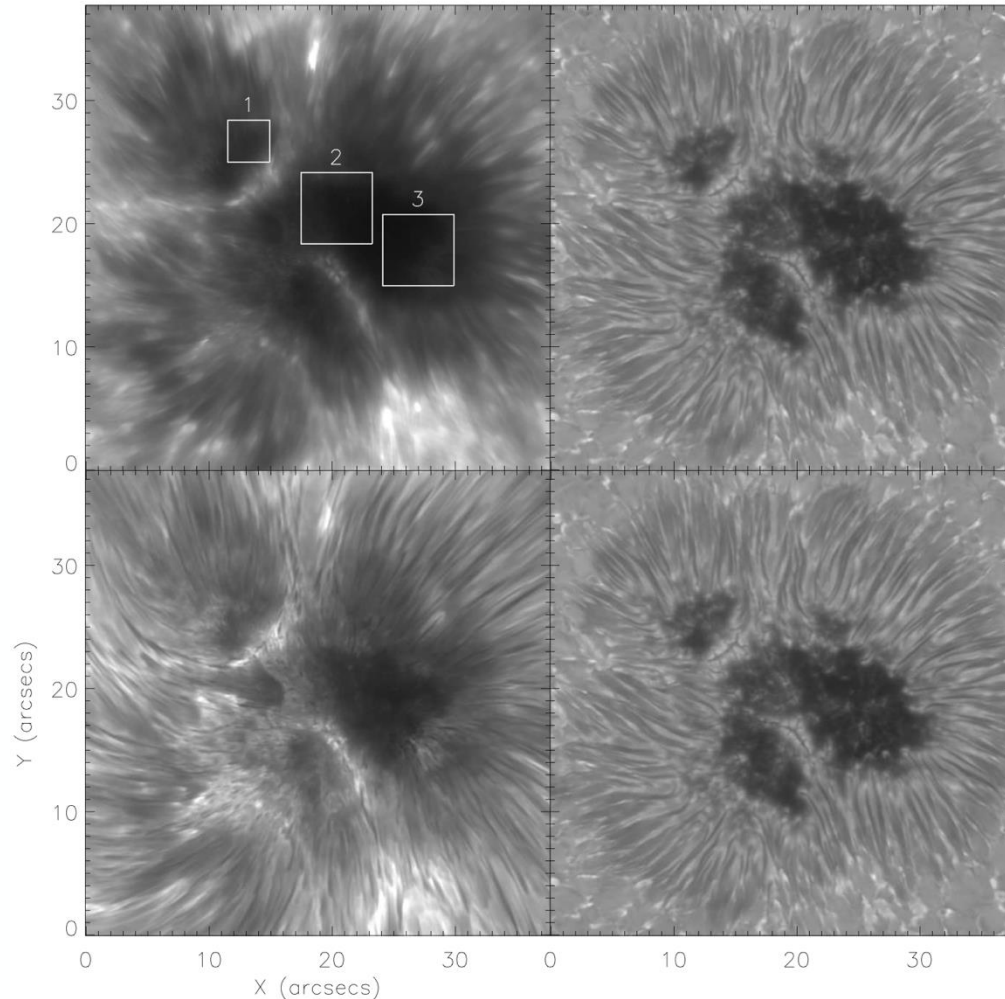
This region is host to one of the longest standing puzzles in astrophysics, namely the 'solar coronal heating problem'. How energy is transported to and dissipated in this region to heat the plasma remains a well-studied and popular mystery.



Credit: Hi-C/NASA

The Solar Atmosphere





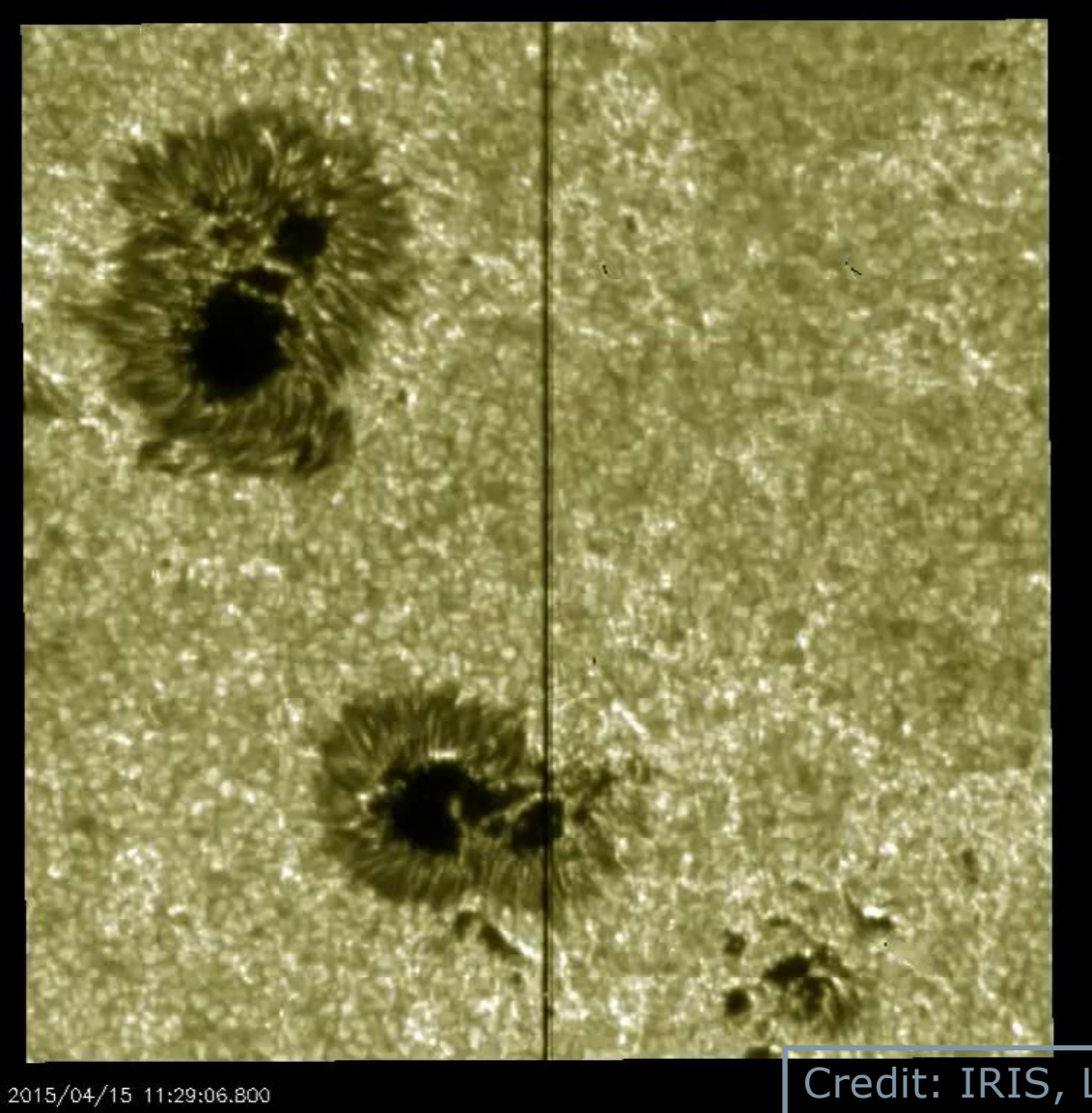
Nelson et al., A&A, 2017

Earth-sized regions of strong magnetic field contained within active regions most clearly seen in the photosphere.

Magnetic field strengths ~ 2000 G
Diameters ~ 20 Mm
Lifetimes \sim Days

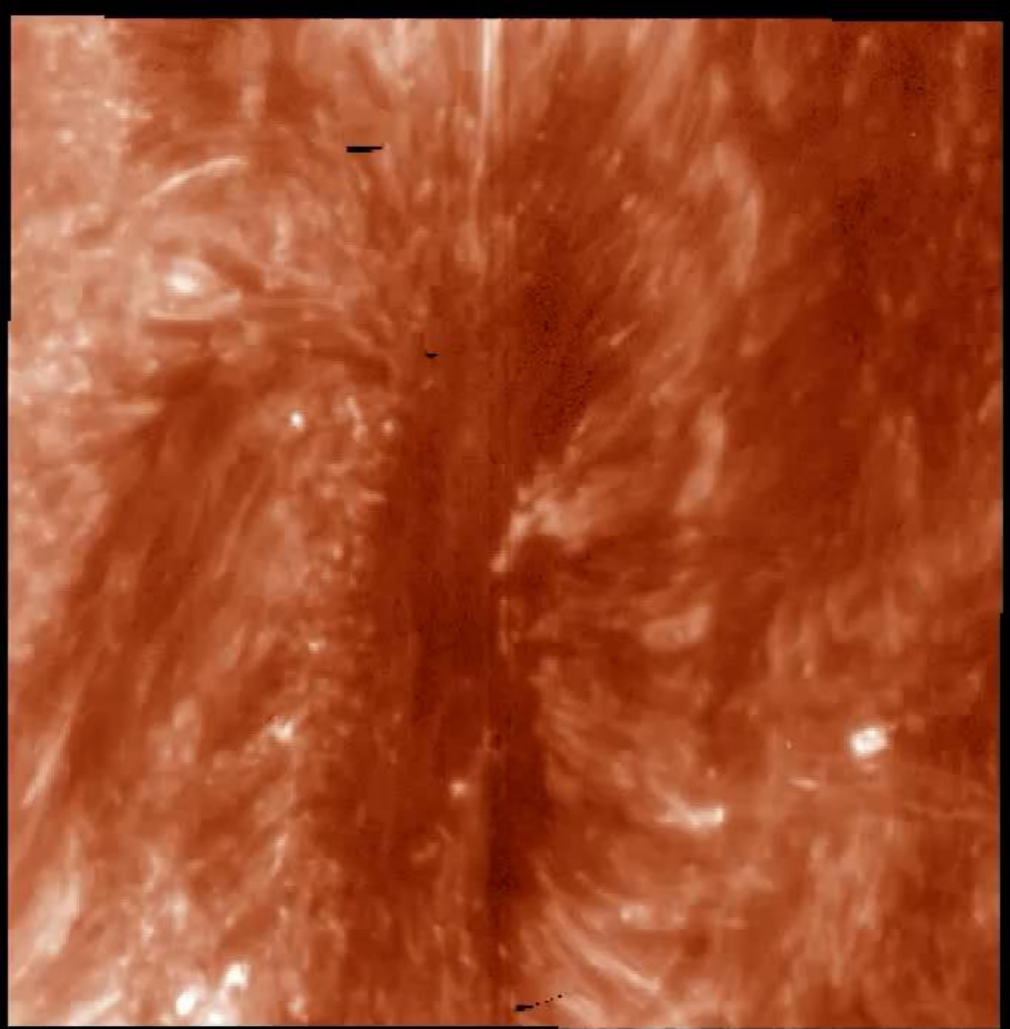
The lower intensity within the sunspot 'umbra' is a result of the strong magnetic field inhibiting convection and, therefore, lowering the local temperature.

Sunspots



Credit: IRIS, LMSAL/NASA, Don Schmit

Sunspots



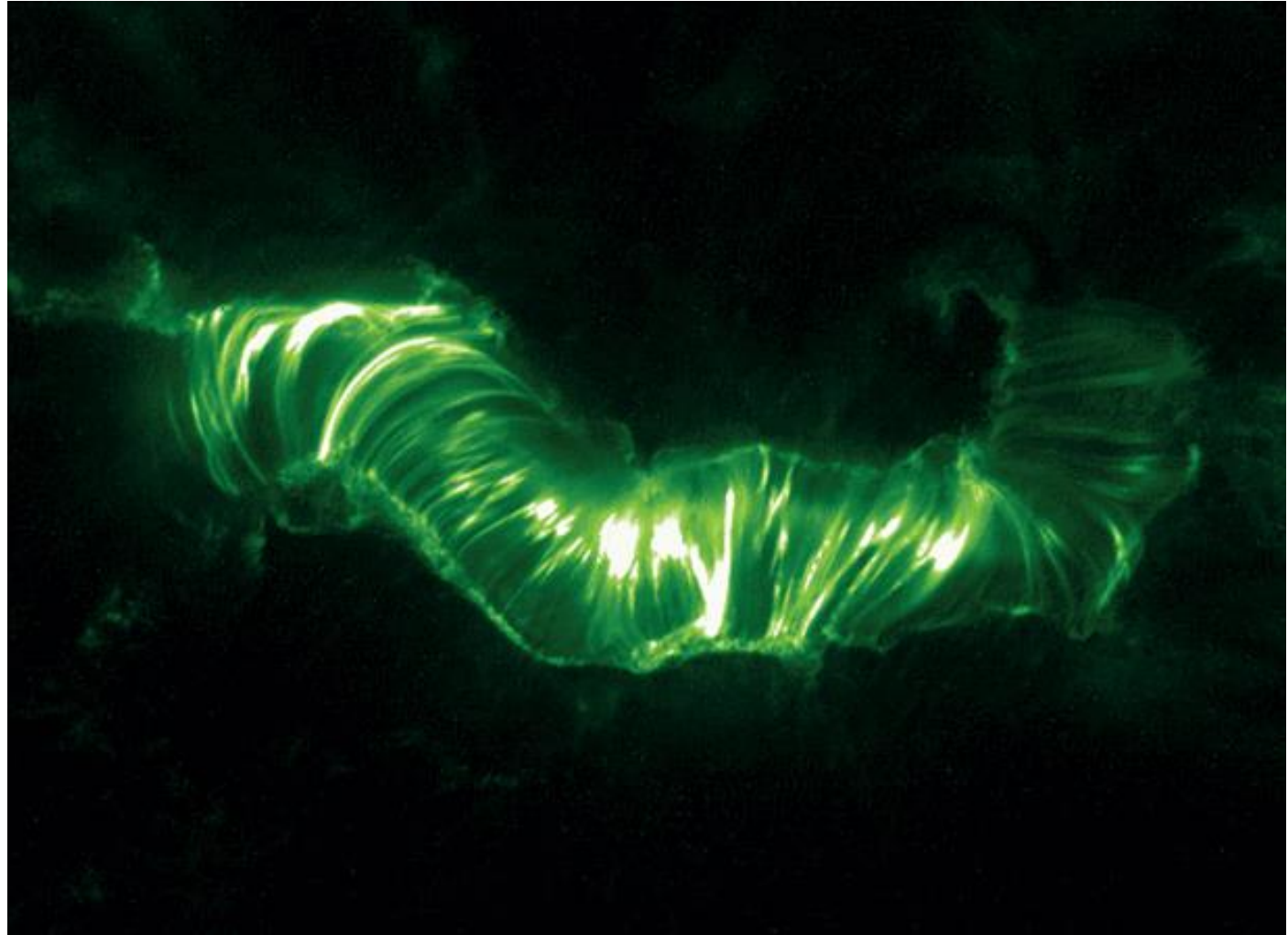
2016/05/25 10:07:01.680

Credit: IRIS, LMSAL/NASA, Wei Liu

Coronal Loops

Long, thin strands of plasma tracking the magnetic field within the corona. These events highlight the connectivity in the upper atmosphere between positive and negative magnetic field regions in the photosphere.

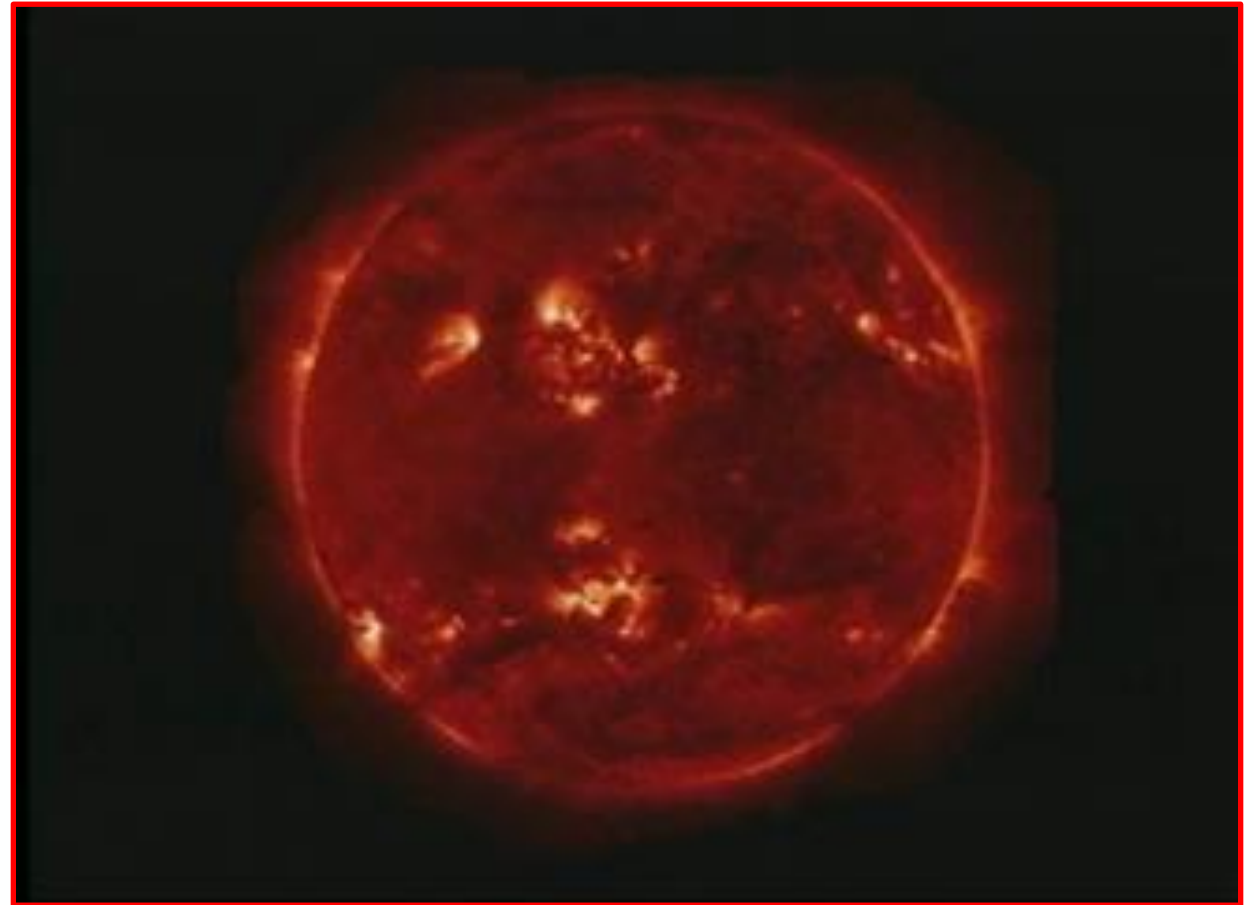
Typical lengths $\sim 100 < \text{Mm}$
Temperatures $\sim 600000 < \text{K}$
Lifetimes $\sim \text{Hours}$



Zaitsev, Geo. & Aero., 2019

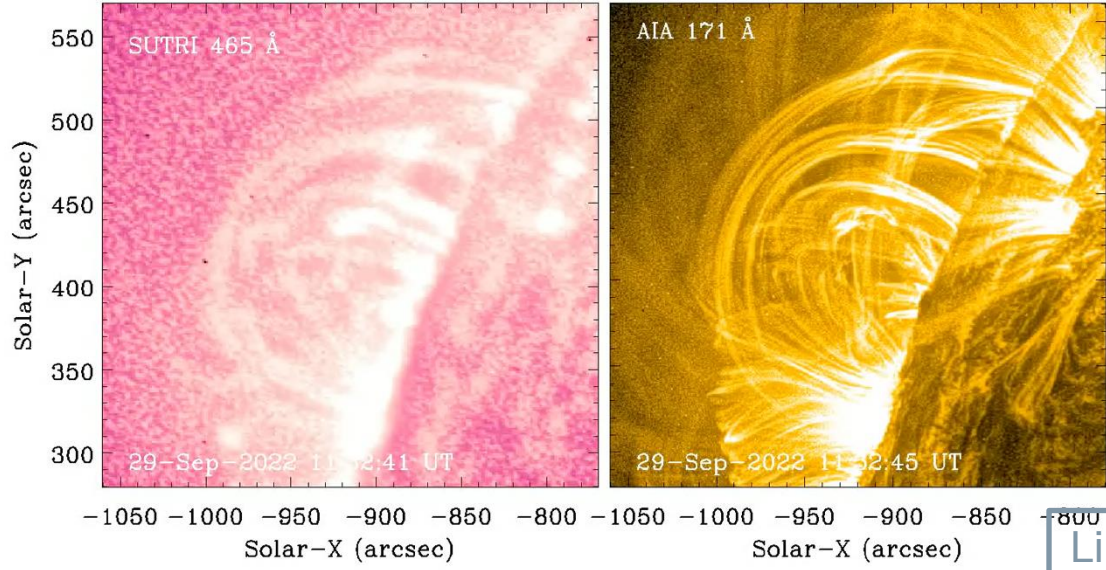
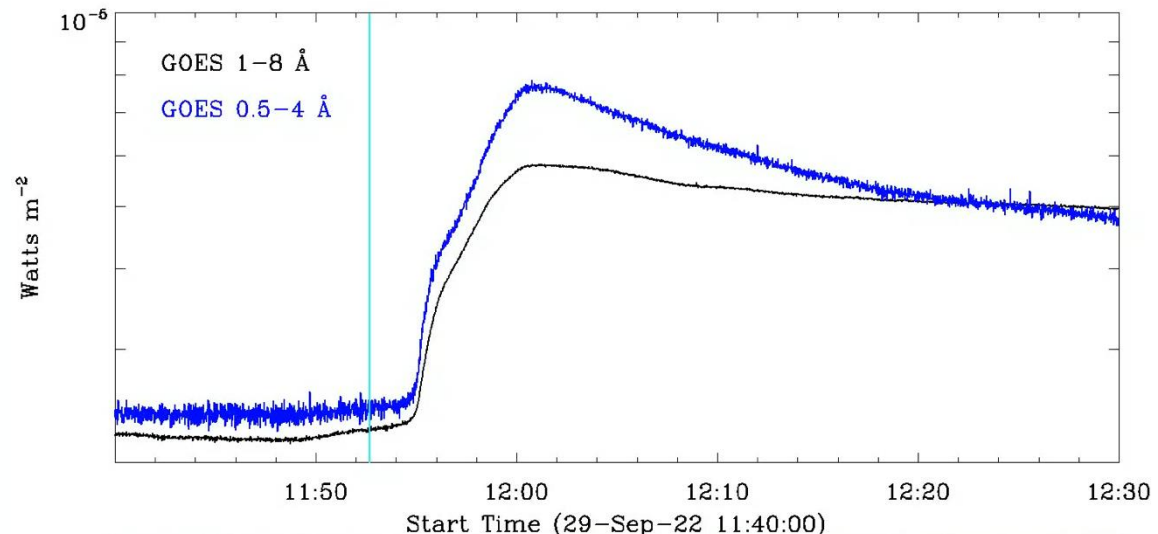
Long, thin strands of plasma tracking the magnetic field within the corona. These events highlight the connectivity in the upper atmosphere between positive and negative magnetic field regions in the photosphere.

Typical lengths $\sim 100 < \text{Mm}$
Temperatures $\sim 600000 < \text{K}$
Lifetimes $\sim \text{Hours}$



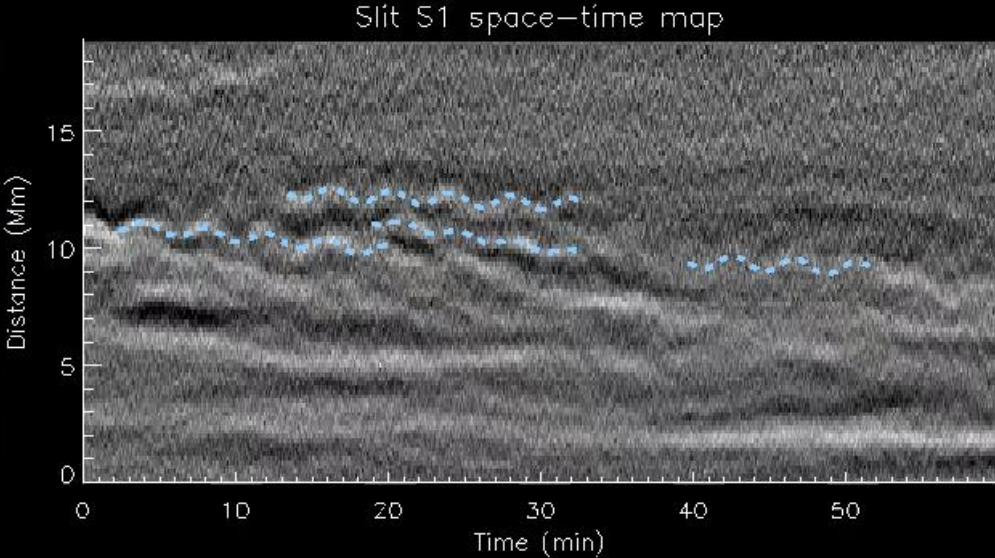
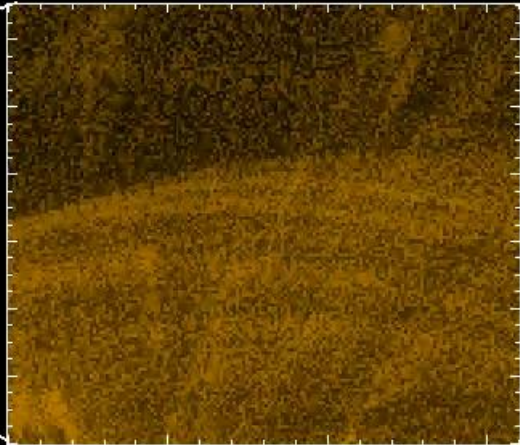
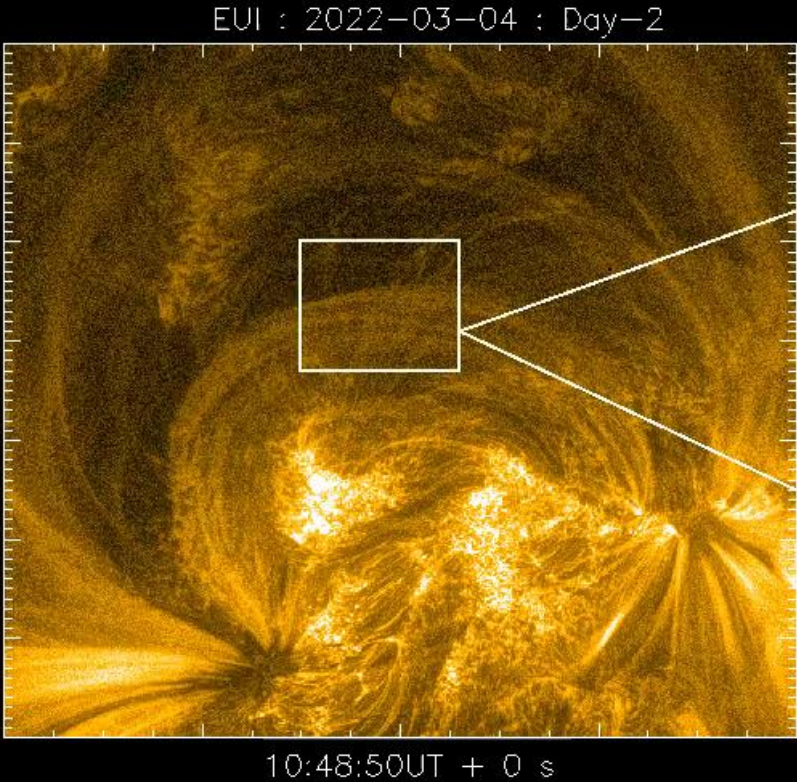
Credit: NASA/TRACE

Coronal Loops



Li et al., A&A, 2021

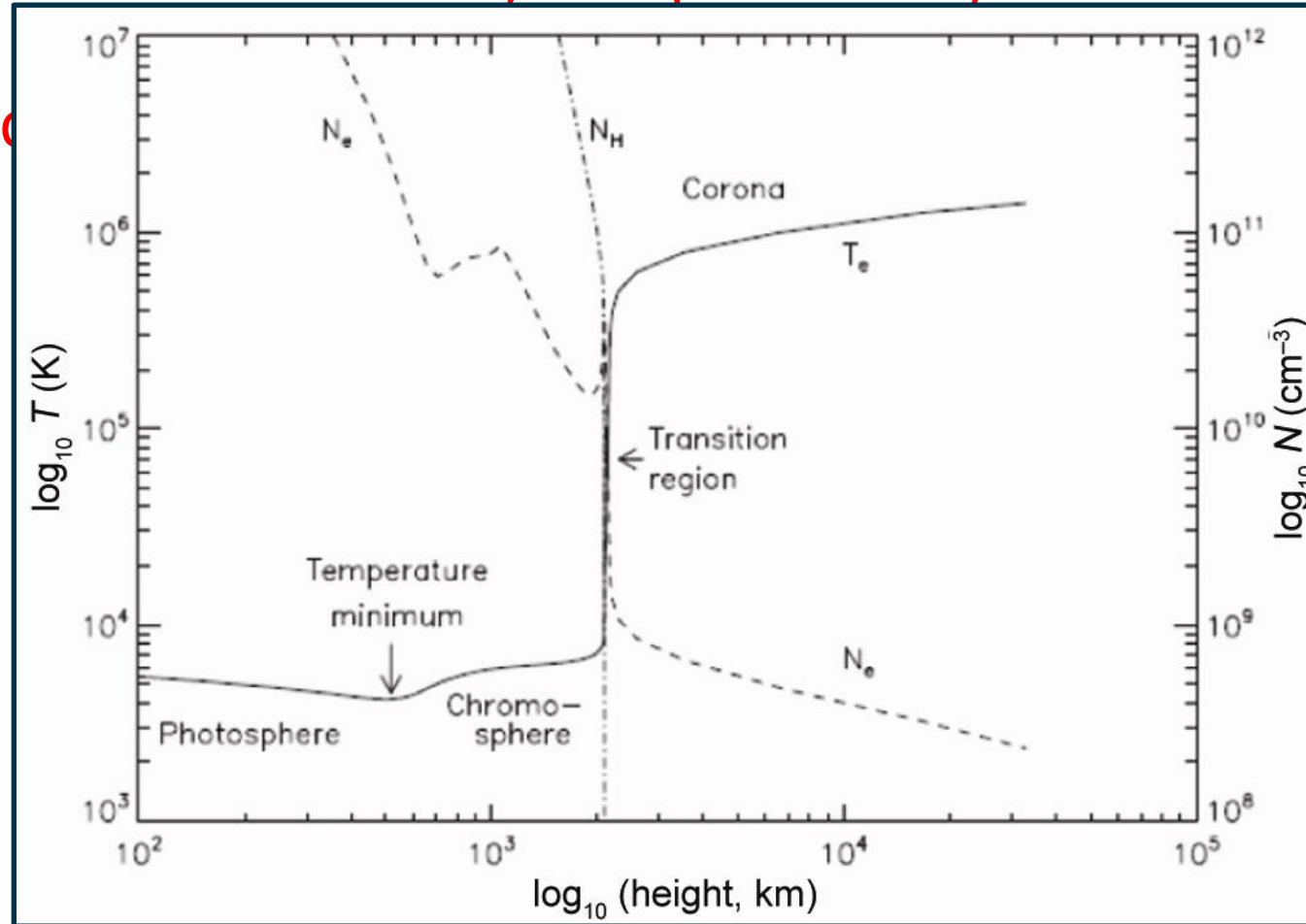
Coronal Loops



Mandal et al., A&A, 2022

- Highly stratified – Densities, temperatures, and other physical parameters vary by several orders of magnitude over distances of tens or hundreds of km

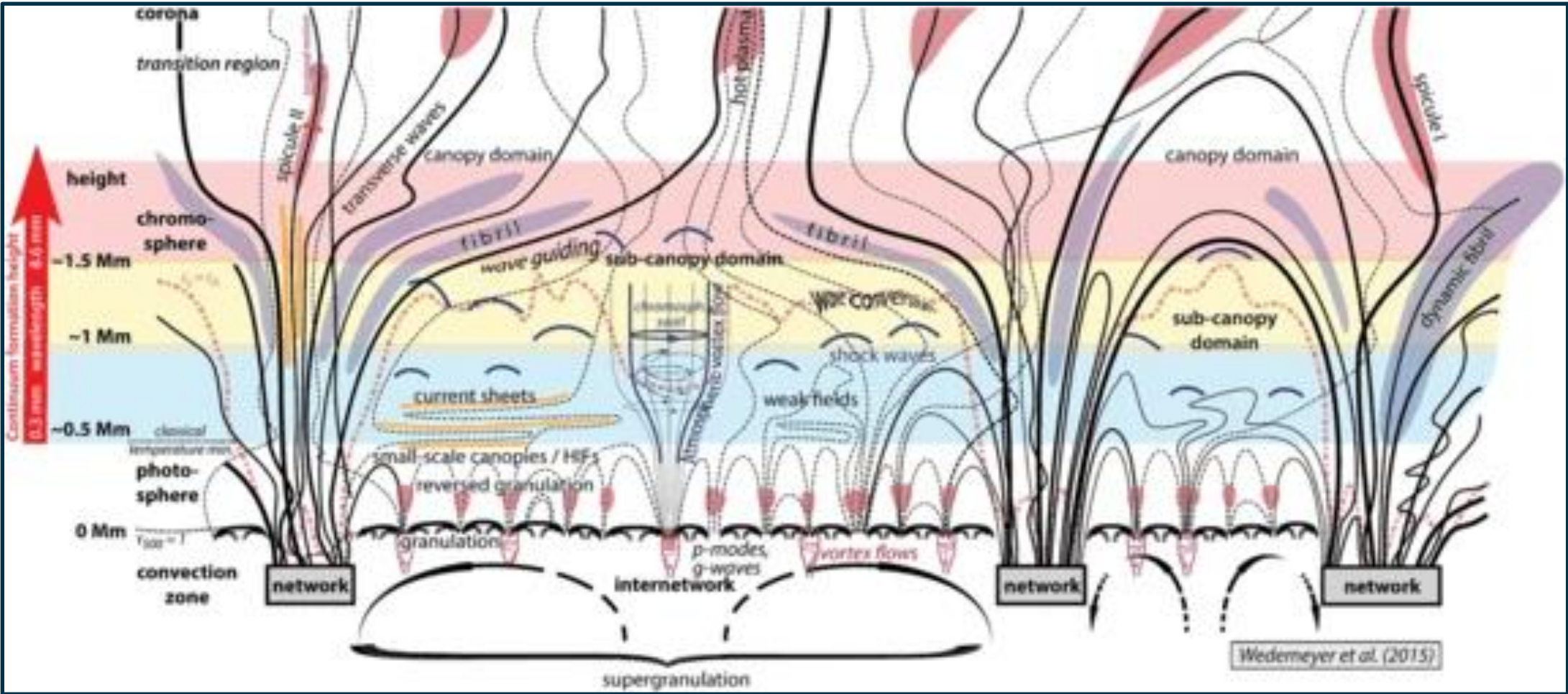
- Highly stratified – Densities, temperatures, and other physical parameters change by tens or hundreds of times over distances of



Aschwanden (2004)

- Highly stratified – Densities, temperatures, and other physical parameters vary by several orders of magnitude over distances of tens or hundreds of km
- Highly structured – Filled with features such as sunspots, spicules, coronal loops.

The Solar Atmosphere

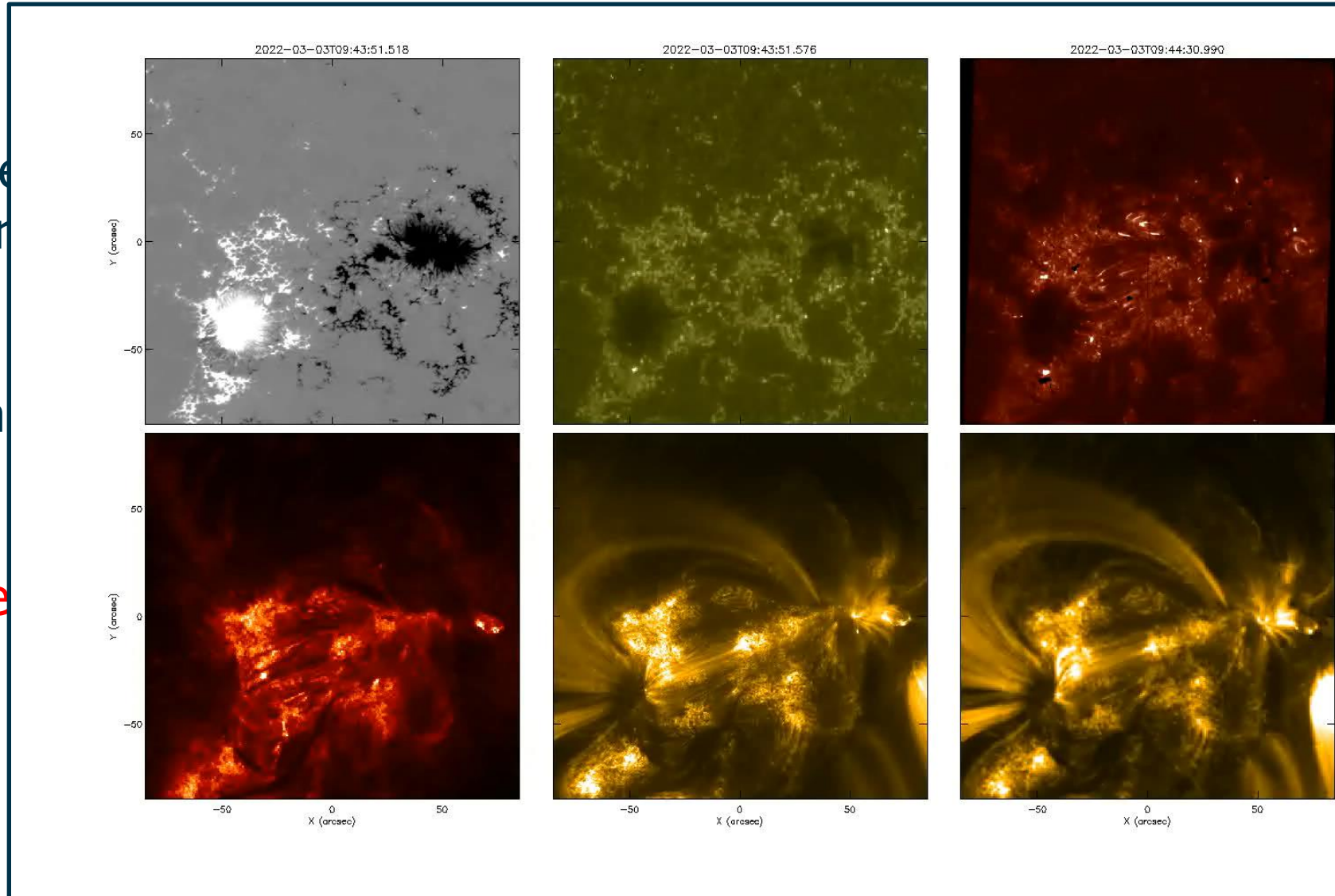


Wedemeyer et al. (2015)

- Highly stratified – Densities, temperatures, and other physical parameters vary by several orders of magnitude over distances of tens or hundreds of km
- Highly structured – Filled with features such as sunspots, spicules, coronal loops.
- Highly dynamic – Structures evolve over time-scales of seconds, minutes, or hours.

The Solar Atmosphere

- Highly parametric
- Highly coronal
- Highly minute



ical
nces of
picules,
onds,

- Highly stratified – Densities, temperatures, and other physical parameters vary by several orders of magnitude over distances of tens or hundreds of km
- Highly structured – Filled with features such as sunspots, spicules, coronal loops.
- Highly dynamic – Structures evolve over time-scales of seconds, minutes, or hours.
- Highly complex – Different physics required to describe the behaviour of the solar atmosphere at different locations.

Introduction to MHD Waves

Geodbloed & Poedts, Principles of Magnetohydrodynamics, 2004

The ideal MHD equations describe the relationships between the magnetic field, velocity, pressure, and density in a plasma.

They apply *only* in specific conditions, namely, in large-scale (relative to the ion gyroradius), slow (relative to the ion gyroperiod) processes in non-relativistic plasmas.

$$\frac{\partial \rho}{\partial t} + \nabla(\rho \mathbf{V}) = 0$$

Mass
Continuity

$$\frac{d}{dt} \left(\frac{P}{\rho^\gamma} \right) = 0$$

Energy
Equation

$$\rho \frac{d\mathbf{V}}{dt} = -\nabla P - \frac{1}{\mu_0} \mathbf{B} \times (\nabla \times \mathbf{B})$$

Euler's
Equation

$$\frac{\partial \mathbf{B}}{\partial t} = \nabla \times (\mathbf{V} \times \mathbf{B})$$

Induction
Equation

$$\nabla \cdot \mathbf{B} = 0$$

Solenoidal
Condition

$$\frac{\partial}{\partial t} = 0$$

$$\mathbf{V} = 0$$

$$\frac{\partial \rho}{\partial t} + \nabla(\rho \mathbf{V}) = 0$$

Mass
Continuity

$$\frac{d}{dt} \left(\frac{P}{\rho^\gamma} \right) = 0$$

Energy
Equation

$$\rho \frac{d\mathbf{V}}{dt} = -\nabla P - \frac{1}{\mu_0} \mathbf{B} \times (\nabla \times \mathbf{B})$$

Euler's
Equation

$$\frac{\partial \mathbf{B}}{\partial t} = \nabla \times (\mathbf{V} \times \mathbf{B})$$

Induction
Equation

$$\nabla \cdot \mathbf{B} = 0$$

Solenoidal
Condition

$$\frac{\partial}{\partial t} = 0$$
$$\mathbf{V} = 0$$

~~$$\frac{\partial \rho}{\partial t} + \nabla(\rho \mathbf{V}) = 0$$~~

Mass
Continuity

~~$$\frac{d}{dt} \left(\frac{P}{\rho^\gamma} \right) = 0$$~~

Energy
Equation

~~$$\rho \frac{d\mathbf{V}}{dt} = -\nabla P - \frac{1}{\mu_0} \mathbf{B} \times (\nabla \times \mathbf{B})$$~~

Euler's
Equation

~~$$\frac{\partial \mathbf{B}}{\partial t} = \nabla \times (\mathbf{V} \times \mathbf{B})$$~~

Induction
Equation

$$\nabla \cdot \mathbf{B} = 0$$

Solenoidal
Condition

We are left with:

$$-\nabla P - \frac{1}{\mu_0} \mathbf{B} \times (\nabla \times \mathbf{B}) = 0$$

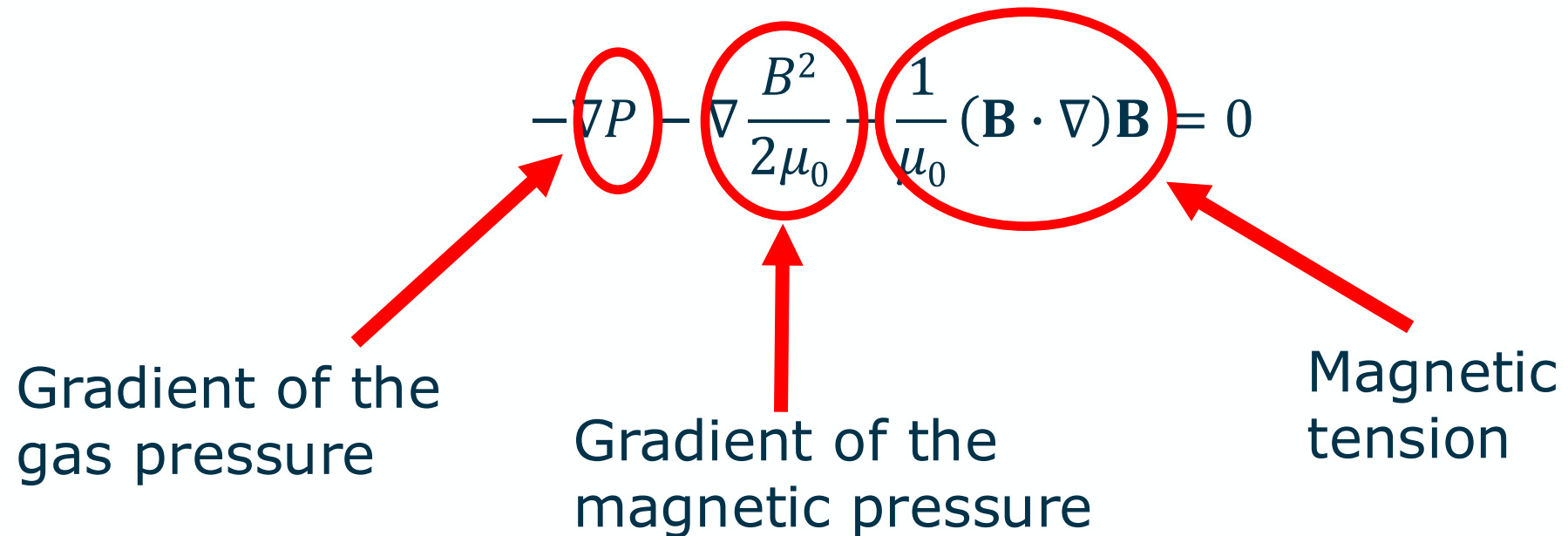
Which can be rewritten as:

$$-\nabla P - \nabla \frac{B^2}{2\mu_0} + \frac{1}{\mu_0} (\mathbf{B} \cdot \nabla) \mathbf{B} = 0$$

We are left with:

$$-\nabla P - \frac{1}{\mu_0} \mathbf{B} \times (\nabla \times \mathbf{B}) = 0$$

Which can be rewritten as:



The diagram shows the equation $-\nabla P - \nabla \frac{B^2}{2\mu_0} - \frac{1}{\mu_0} (\mathbf{B} \cdot \nabla) \mathbf{B} = 0$. Three terms are circled in red: $-\nabla P$, $\nabla \frac{B^2}{2\mu_0}$, and $\frac{1}{\mu_0} (\mathbf{B} \cdot \nabla) \mathbf{B}$. Red arrows point from these terms to labels below: 'Gradient of the gas pressure' for $-\nabla P$, 'Gradient of the magnetic pressure' for $\nabla \frac{B^2}{2\mu_0}$, and 'Magnetic tension' for $\frac{1}{\mu_0} (\mathbf{B} \cdot \nabla) \mathbf{B}$.

$$-\nabla P - \nabla \frac{B^2}{2\mu_0} - \frac{1}{\mu_0} (\mathbf{B} \cdot \nabla) \mathbf{B} = 0$$

Gradient of the gas pressure

Gradient of the magnetic pressure

Magnetic tension

If we calculate the ratio of the gas and magnetic pressures, we obtain a value known as the 'plasma beta':

$$\beta \equiv \frac{P}{B^2/2\mu_0}$$

This term, essentially, tells us whether the gas or the magnetic field is the dominant mechanism in a specific region of plasma. Rewriting this term such that:

$$\beta = 3.5 \times 10^{-21} n T B^{-2}$$

allows us to estimate the plasma beta in specific regions.

In a granule: $n = 10^{23} \text{ m}^{-3}$, $T = 6000 \text{ K}$, and $B = 100 \text{ G}$ returns $\beta = 210$

In a sunspot: $n = 10^{23} \text{ m}^{-3}$, $T = 6000 \text{ K}$, and $B = 2000 \text{ G}$ returns $\beta = 0.5$

$$\frac{\partial \rho}{\partial t} + \nabla(\rho \mathbf{V}) = 0$$

$$\frac{d}{dt} \left(\frac{P}{\rho^\gamma} \right) = 0$$

$$\begin{aligned} & \rho \frac{d\mathbf{V}}{dt} \\ &= -\nabla P - \frac{1}{\mu_0} \mathbf{B} \times (\nabla \times \mathbf{B}) \\ &= \nabla \times (\mathbf{V} \times \mathbf{B}) \end{aligned}$$

$$\frac{\partial \rho}{\partial t} + \nabla(\rho \mathbf{V}) = 0$$

$$\frac{d}{dt} \left(\frac{P}{\rho^\gamma} \right) = 0$$

$$\begin{aligned} \rho \frac{d\mathbf{V}}{dt} &= -\nabla P - \frac{1}{\mu_0} \mathbf{B} \times (\nabla \times \mathbf{B}) \\ &= \nabla \times (\mathbf{V} \times \mathbf{B}) \end{aligned}$$

ASSUMPTIONS

No stratification – The density and pressure are constant everywhere

No structuring – The magnetic field is purely vertical and is constant everywhere

$$\frac{\partial \rho}{\partial t} + \nabla(\rho \mathbf{V}) = 0$$

$$\frac{d}{dt} \left(\frac{P}{\rho^\gamma} \right) = 0$$



$$\mathbf{B} = \mathbf{B}_0 + \mathbf{B}_1(r, t)$$

$$\mathbf{V} = \mathbf{0} + \mathbf{V}_1(r, t)$$

$$P = P_0 + P_1(r, t)$$

$$\rho = \rho_0 + \rho_1(r, t)$$

$$\begin{aligned} & \rho \frac{d\mathbf{V}}{dt} \\ &= -\nabla P - \frac{1}{\mu_0} \mathbf{B} \times (\nabla \times \mathbf{B}) \\ & \quad \frac{\partial \mathbf{B}}{\partial t} \\ &= \nabla \times (\mathbf{V} \times \mathbf{B}) \end{aligned}$$

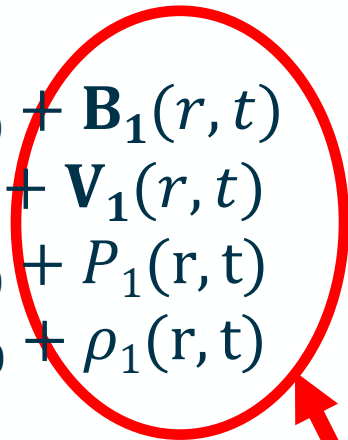
$$\frac{\partial \rho}{\partial t} + \nabla(\rho \mathbf{V}) = 0$$

$$\frac{d}{dt} \left(\frac{P}{\rho^\gamma} \right) = 0$$

$$\begin{aligned} \rho \frac{d\mathbf{V}}{dt} &= -\nabla P - \frac{1}{\mu_0} \mathbf{B} \times (\nabla \times \mathbf{B}) \\ &= \nabla \times (\mathbf{V} \times \mathbf{B}) \end{aligned}$$



$$\begin{aligned} \mathbf{B} &= \mathbf{B}_0 + \mathbf{B}_1(r, t) \\ \mathbf{V} &= \mathbf{0} + \mathbf{V}_1(r, t) \\ P &= P_0 + P_1(r, t) \\ \rho &= \rho_0 + \rho_1(r, t) \end{aligned}$$



Assume these perturbations are small

$$\frac{\partial \rho}{\partial t} + \nabla(\rho \mathbf{V}) = 0$$

$$\frac{d}{dt} \left(\frac{P}{\rho^\gamma} \right) = 0$$

$$\begin{aligned} \rho \frac{d\mathbf{V}}{dt} &= -\nabla P - \frac{1}{\mu_0} \mathbf{B} \times (\nabla \times \mathbf{B}) \\ &= \nabla \times (\mathbf{V} \times \mathbf{B}) \end{aligned}$$



$$\begin{aligned} \mathbf{B} &= \mathbf{B}_0 + \mathbf{B}_1(r, t) \\ \mathbf{V} &= \mathbf{0} + \mathbf{V}_1(r, t) \\ P &= P_0 + P_1(r, t) \\ \rho &= \rho_0 + \rho_1(r, t) \end{aligned}$$



$$\begin{aligned} \frac{\partial \rho_1}{\partial t} + \rho_0 \nabla \mathbf{V}_1 &= 0 \\ \frac{\partial P_1}{\partial t} - \frac{\gamma P_0}{\rho_0} \frac{\partial \rho_1}{\partial t} &= 0 \\ \rho_0 \frac{d\mathbf{V}_1}{dt} &= -\nabla P_1 - \frac{1}{\mu_0} \mathbf{B}_0 \times (\nabla \times \mathbf{B}_1) \\ \frac{\partial \mathbf{B}_1}{\partial t} &= \nabla \times (\mathbf{V}_1 \times \mathbf{B}_0) \end{aligned}$$

$$\frac{\partial \rho_1}{\partial t} + \rho_0 \nabla \mathbf{V}_1 = 0$$

$$\frac{\partial P_1}{\partial t} - \frac{\gamma P_0}{\rho_0} \frac{\partial \rho_1}{\partial t} = 0$$

$$\rho_0 \frac{d\mathbf{V}_1}{dt} = -\nabla P_1 - \frac{1}{\mu_0} \mathbf{B}_0 \times (\nabla \times \mathbf{B}_1)$$

$$\frac{\partial \mathbf{B}_1}{\partial t} = \nabla \times (\mathbf{V}_1 \times \mathbf{B}_0)$$

Let us assume we have a straight magnetic field in the xz-plane and plane waves propagating in the z-direction, such that:

$$\mathbf{B}_0 = B_0 \sin \alpha \mathbf{e}_x + B_0 \cos \alpha \mathbf{e}_z,$$

$$\frac{\partial}{\partial t} \rightarrow -i\omega,$$

$$\nabla \rightarrow ik.$$

$$-i\omega\rho_1 + ik\rho_0V_{z1} = 0,$$

$$-i\omega\rho_0V_{x1} - \frac{ikB_0\cos\alpha}{\mu_0}B_{x1} = 0,$$

$$-i\omega\rho_0V_{y1} - \frac{ikB_0\cos\alpha}{\mu_0}B_{y1} = 0,$$

$$-i\omega\rho_0V_{z1} + ikP_1 + \frac{ikB_0\sin\alpha}{\mu_0}B_{x1} = 0,$$

$$-i\omega B_{x1} + ikB_0\sin\alpha V_{z1} - ikB_0\cos\alpha V_{x1} = 0,$$

$$-i\omega B_{y1} + ikB_0\cos\alpha V_{y1} = 0,$$

$$-i\omega B_{z1} = 0,$$

$$-i\omega P_1 - \frac{i\omega\gamma P_0}{\rho_0}\rho_1 = 0,$$

$$-i\omega\rho_1 + ik\rho_0V_{z1} = 0,$$

$$-i\omega\rho_0V_{x1} - \frac{ikB_0\cos\alpha}{\mu_0}B_{x1} = 0,$$

$$-i\omega\rho_0V_{y1} - \frac{ikB_0\cos\alpha}{\mu_0}B_{y1} = 0,$$

$$-i\omega\rho_0V_{z1} + ikP_1 + \frac{ikB_0\sin\alpha}{\mu_0}B_{x1} = 0,$$

$$-i\omega B_{x1} + ikB_0\sin\alpha V_{z1} - ikB_0\cos\alpha V_{x1} = 0,$$

$$-i\omega B_{y1} + ikB_0\cos\alpha V_{y1} = 0,$$

$$-i\omega B_{z1} = 0,$$

$$-i\omega P_1 - \frac{i\omega\gamma P_0}{\rho_0}\rho_1 = 0,$$

Terms in the y-direction *decouple* returning:

$$\omega^2 - CA^2\cos^2\alpha k^2 = 0$$

where $C_A^2 = \frac{B_0^2}{(\mu_0\rho_0)}$ is the square of the *Alfvén speed*.

This is the dispersion relation for **Alfvén waves**.

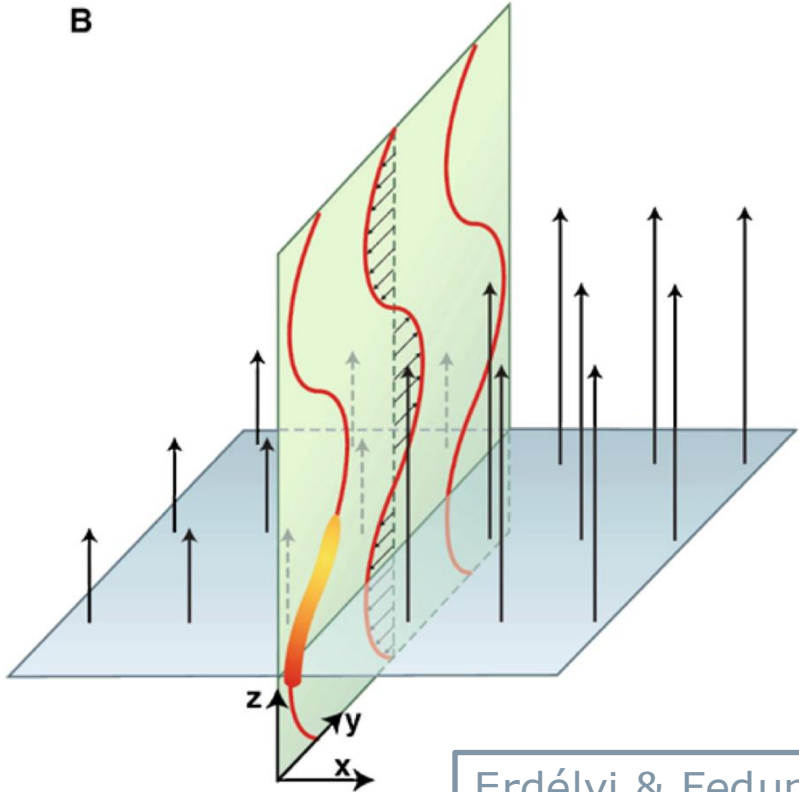
$$\omega^2 - CA^2 \cos^2 \alpha k^2 = 0$$

Key take-homes:

- Transverse waves – perpendicular to **k**.
- Only dependent on the magnetic field – no gas pressure terms.
- Non-compressible – no ability to perturb the density.
- Do not perturb the axis of the host structure.

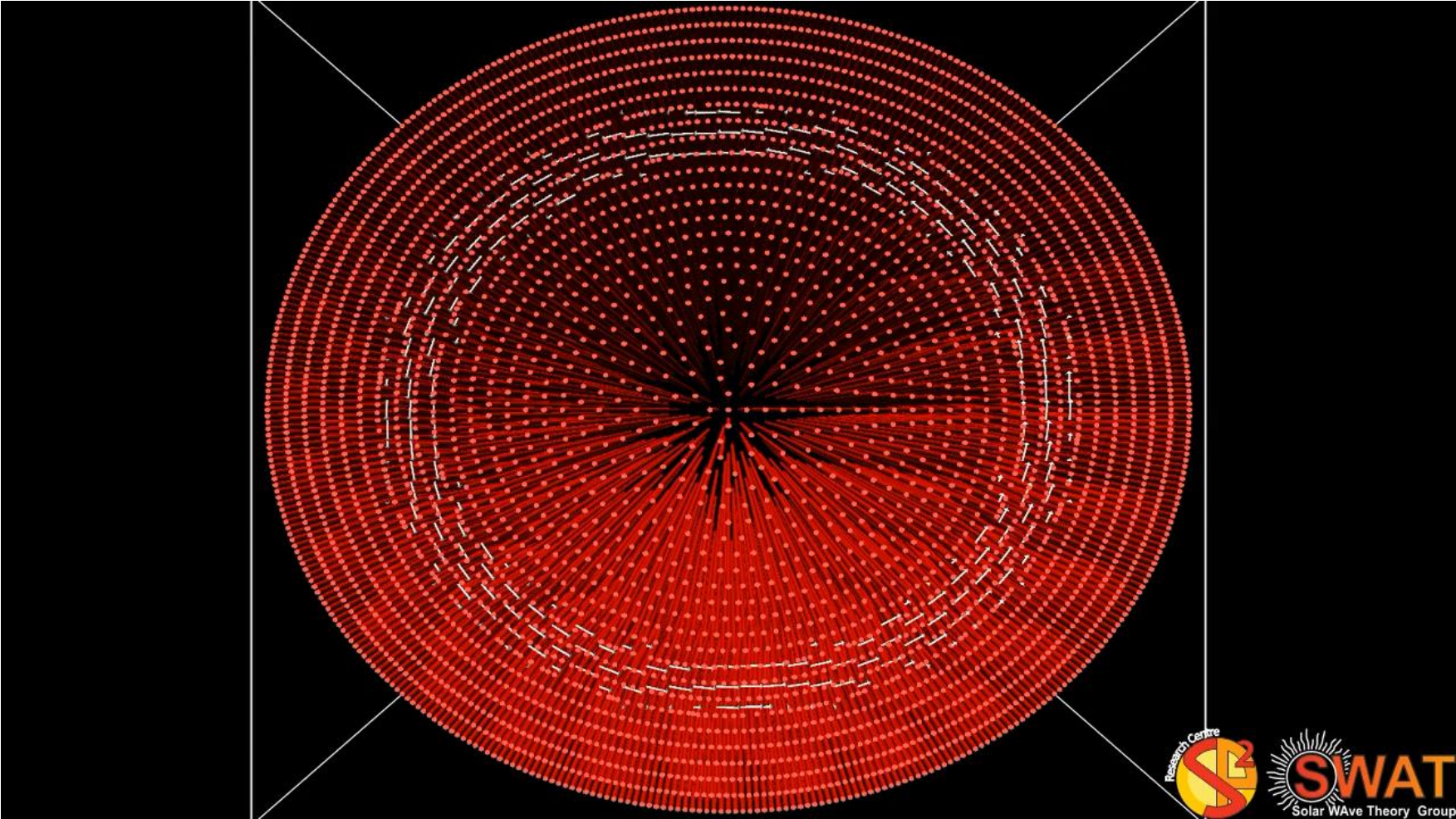
Combined, these facts make Alfvén waves *extremely* difficult to observe.

$$\omega^2 - CA^2 \cos^2 \alpha k^2 = 0$$



Erdélyi & Fedun, Science, 2007

Alfvén Waves – Cylindrical Geometry



Torsional oscillations within a magnetic pore in the solar photosphere

Marco Stangalini^{1,2}, Robertus Erdélyi^{3,4,5}, Callum Boocock⁶, David Tsiklauri⁶, Christopher J. Nelson⁷, Dario Del Moro⁸, Francesco Berrilli⁸ and Marianna B. Korsós^{3,4,9}

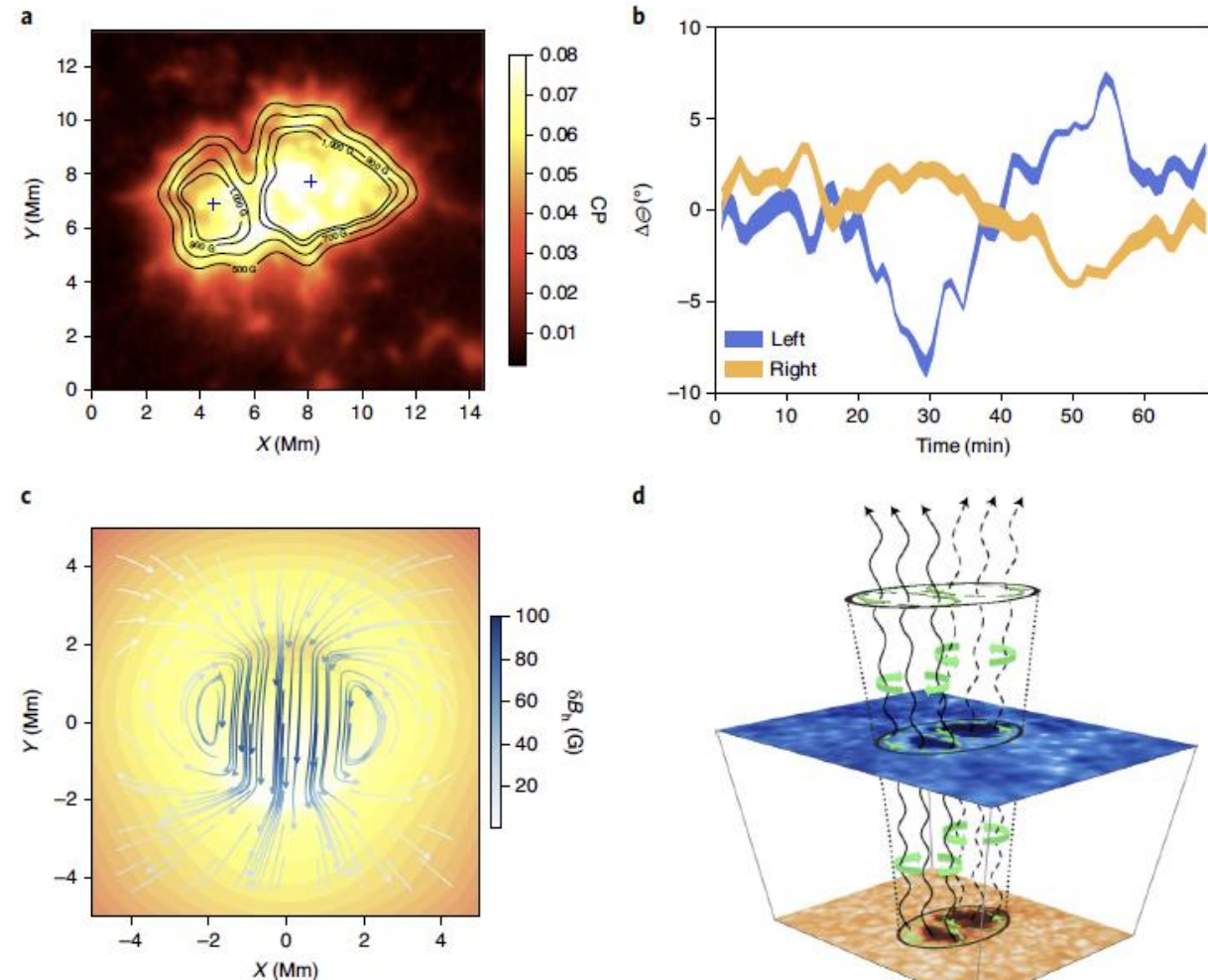
Alfvén waves have proven to be important in a range of physical systems due to their ability to transport non-thermal energy over long distances in a magnetized plasma. This property is of specific interest in solar physics, where the extreme heating of the atmosphere of the Sun remains unexplained. In an inhomogeneous plasma such as a flux tube in the solar atmosphere, they manifest as incompressible torsional perturbations. However, despite evidence in the upper atmosphere, they have not been directly observed in the photosphere. Here, we report the detection of antiphase incompressible torsional oscillations observed in a magnetic pore in the photosphere by the Interferometric Bidimensional Spectropolarimeter. State-of-the-art numerical simulations suggest that a kink mode is a possible excitation mechanism of these waves. The excitation of torsional waves in photospheric magnetic structures can substantially contribute to the energy transport in the solar atmosphere and the acceleration of the solar wind, especially if such signatures will be ubiquitously detected in even smaller structures with the forthcoming next generation of solar telescopes.

The existence of Alfvén waves was predicted theoretically more than 70 years ago¹ and they were immediately recognized for their potential impact in many research areas, including neutrino physics², the heating of the solar upper atmosphere—the corona—to million-degree temperatures^{3,4}, protostellar disks⁵, the physics of the interstellar medium⁶, particle acceleration around supermassive black holes⁷ and nuclear fusion research, where these magnetic waves have been proposed as a possible effective heating mechanism in tokamaks^{8,9}.

One of the fundamental major applications in plasma physics is that torsional waves play a key role in the transportation and dissipation of energy, potentially leading to heating. Examples where these properties could be important include both laboratory and space plasmas, such as the intergalactic medium, plasma fusion reactors or the solar atmosphere from the chromosphere to the corona. In solar magnetic flux tubes, these waves manifest as either axisymmetric or antisymmetric torsional perturbations¹⁰ (torsional Alfvén waves; hereafter TAWs), which have magnetic tension as their sole restoring force. A number of studies have presented a range of indirect confirmations of Alfvén wave manifestation¹¹ over the past decades, including counter-flowing velocities on opposite sides of solar jets and perturbations to spectral linewidths. These earlier studies were limited mostly to the upper solar atmosphere^{12,13} and solar wind¹⁴, meaning that no observation of torsional motion that could be linked to TAWs¹⁵ has been directly detected in the photosphere. Therefore, Alfvén waves remain the most elusive, yet physically intriguing, class of magnetohydrodynamic (MHD) waves, and are still waiting to be fully understood despite decades of research.

Spectropolarimetry has long been a standard method used to infer magnetic fields in the Sun and other stars; however, the spatial, temporal and spectral resolutions we can now achieve with

observations of our nearest star mean that the polarimetric footprint left by the magnetic field in the Sun's photospheric plasma can now be exploited to map and study its magnetic structures and their associated dynamics in fine detail. Specifically, the high temporal and spatial resolutions (scales close to 120 km on the surface of the Sun can be sampled a few times every minute) achieved by modern two-dimensional solar spectropolarimetric imagers such as the Interferometric Bidimensional Spectropolarimeter (IBIS)¹⁶, the two-dimensional spectropolarimeter at the Dunn Solar Telescope (New Mexico, USA), are perfect for studying the fine structure and rapid dynamical behaviour of photospheric magnetic structures such as pores. The instantaneous circular polarization (CP) map of the light emerging from the pore studied here in the magnetically sensitive Fe I 617.3 nm spectral line is plotted in Fig. 1a. This represents a direct indicator of the vertical magnetic field of the structure at this time. The ~69 min duration and 52 s temporal resolution of the IBIS dataset studied here allow us to investigate the evolution of the entire magnetic structure and, specifically, to trace torsional magnetic oscillations, perpendicular to the line of sight, through time. To achieve this, we initially transform the temporal sequence of CP maps into polar coordinates (see Supplementary Fig. 1 for an example). The approximate positions of the centres of the two magnetic lobes (marked by the two crosses in Fig. 1a) are employed as the radial origins of the structures. Overplotted on Fig. 1a are the streamlines of the torsional oscillations with azimuthal wave number $m=1$, indicating its dipolar nature. The measured angular shifts of both lobes, as a function of time, are shown in Fig. 1b, where it is simple to recognize a periodic angular displacement in both sides of the pore. It is worth noting that the torsional oscillations of the two lobes are out of phase. The thickness of the curves indicates the 3σ error associated with the measures (see Methods for more details).



¹ASI, Italian Space Agency, Rome, Italy. ²INAF-OAR, National Institute for Astrophysics, Monte Porzio Catone, Italy. ³Solar Physics and Space Plasma Research Centre (SP2RC), School of Mathematics and Statistics, The University of Sheffield, Sheffield, UK. ⁴Department of Astronomy, Eötvös Loránd University, Budapest, Hungary. ⁵Gyula Bay Zoltán Solar Observatory (GSO), Hungarian Solar Physics Foundation (HSPF), Gyula, Hungary. ⁶School of Physics and Astronomy, Queen Mary University of London, London, UK. ⁷Astrophysics Research Centre (ARC), School of Mathematics and Physics, Queen's University, Belfast, UK. ⁸Department of Physics, University of Rome Tor Vergata, Rome, Italy. ⁹Department of Physics, Aberystwyth University, Aberystwyth, UK. ¹⁰email: marco.stangalini@asi.it; robertus@sheffield.ac.uk

Manipulating the other linearised MHD equations gives:

$$(\omega^2 - CA^2 \cos^2 \alpha k^2)(\omega^2 - CS^2 k^2) - CA^2 \sin^2 \alpha \omega^2 k^2 = 0$$

where $C_S^2 = \left(\frac{\gamma P_0}{\rho_0}\right)$ is the square of the *sound speed*. This 4th order equation has two pairs of solutions corresponding to *slow* and *fast* magnetoacoustic waves.

Manipulating the other linearised MHD equations gives:

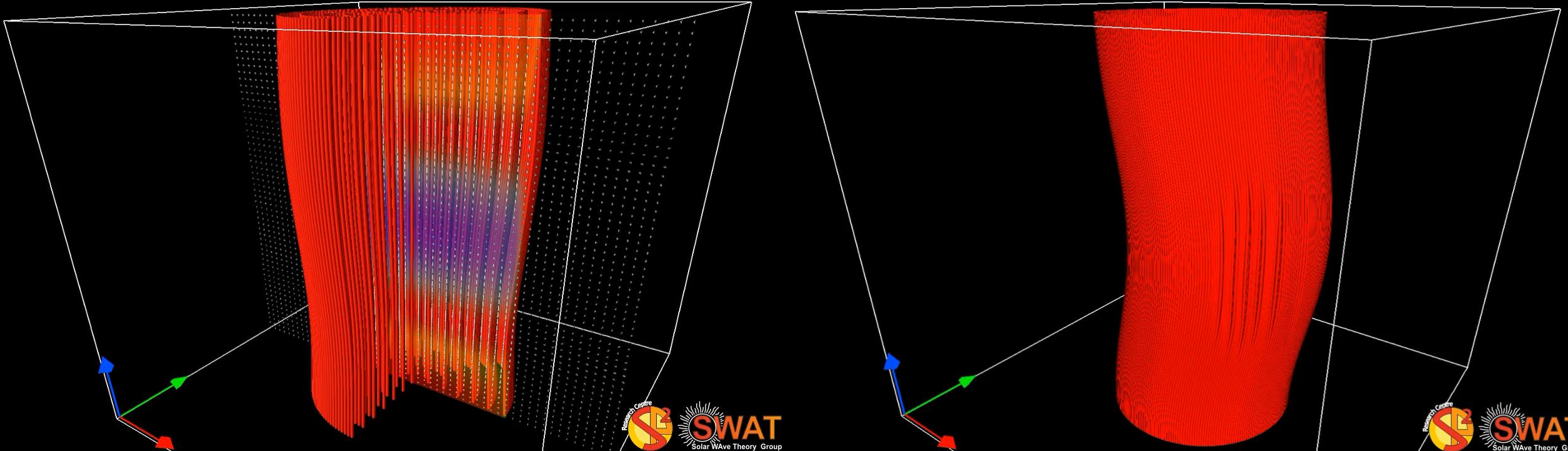
$$(\omega^2 - CA^2 \cos^2 \alpha k^2)(\omega^2 - CS^2 k^2) - CA^2 \sin^2 \alpha \omega^2 k^2 = 0$$

where $C_s^2 = \left(\frac{\gamma P_0}{\rho_0}\right)$ is the square of the *sound speed*. This 4th order equation has two pairs of solutions corresponding to *slow* and *fast* magnetoacoustic waves.

Key take-homes:

- Longitudinal waves – parallel to \mathbf{k} .
- Both magnetic and gas pressure terms – return to acoustic waves if $\mathbf{B}_0 = 0$.
- Highly compressible.
- Ability to perturb the axis of the host structure.

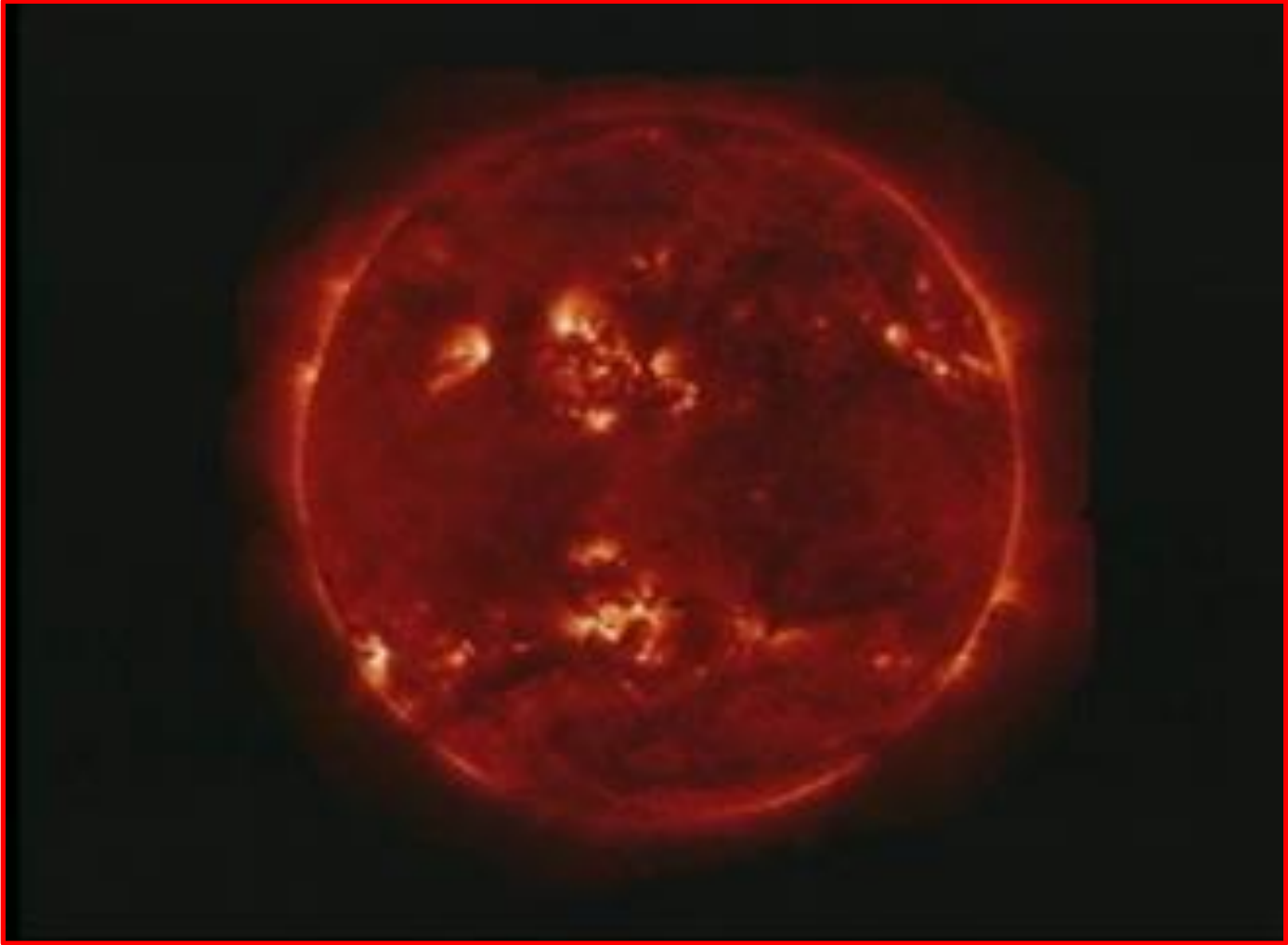
Magnetoacoustic Waves – Cylindrical Geometry



Sausage mode

Kink mode

Magnetoacoustic Waves – Cylindrical Geometry



Credit: NASA/TRACE

Apply MHD equations in different geometries including other effects such as cooling, twist, partial ionisation

Apply MHD equations in different geometries including other effects such as cooling, twist, partial ionisation



Derive properties of different wave types

Apply MHD equations in different geometries including other effects such as cooling, twist, partial ionisation



Derive properties of different wave types



Compare these to observations of waves in the solar atmosphere

Apply MHD equations in different geometries including other effects such as cooling, twist, partial ionisation



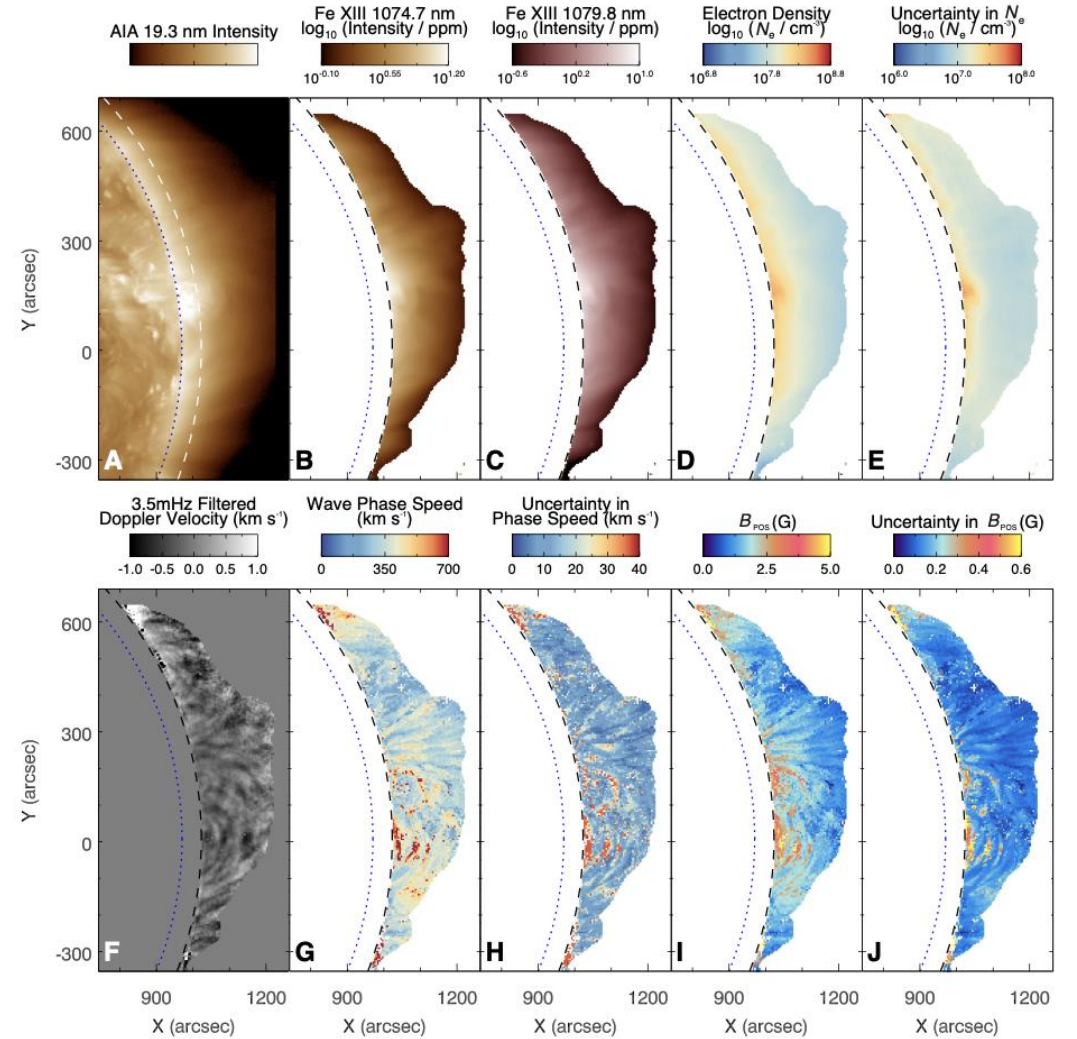
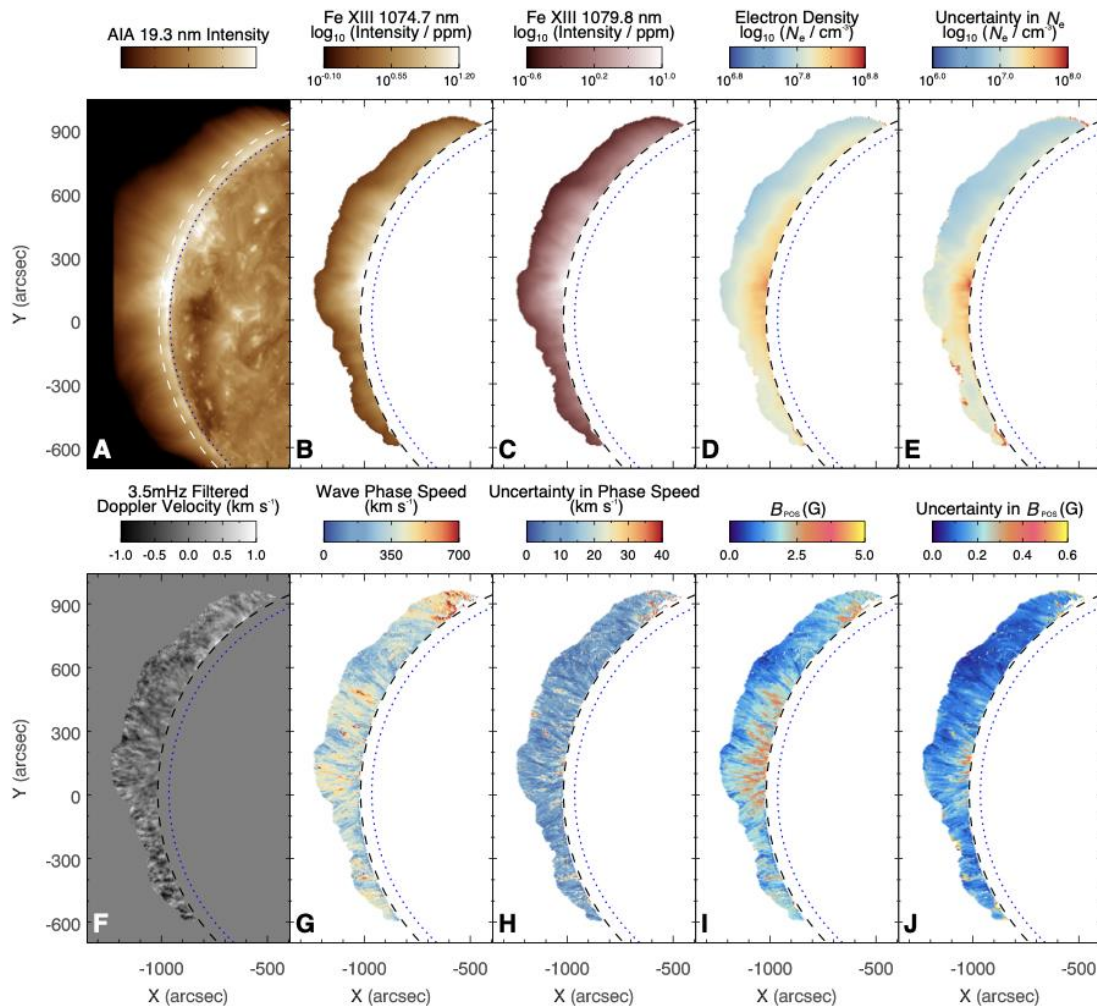
Derive properties of different wave types



Compare these to observations of waves in the solar atmosphere

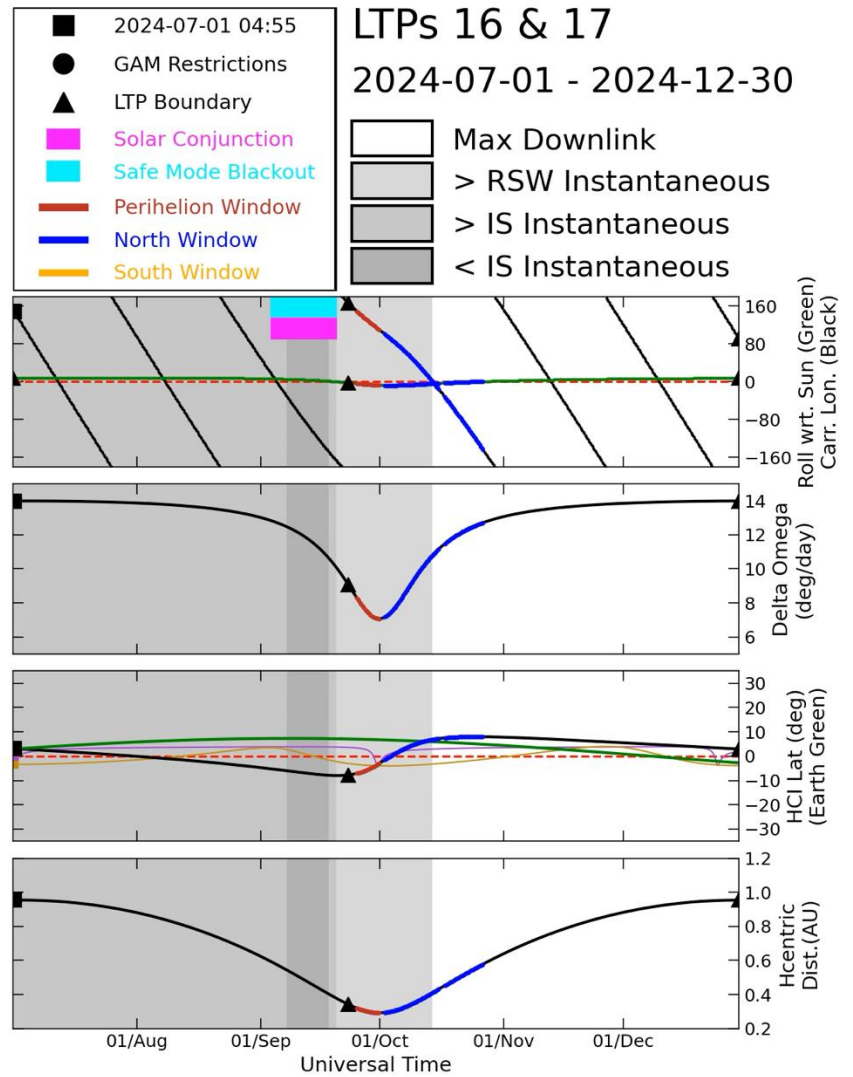
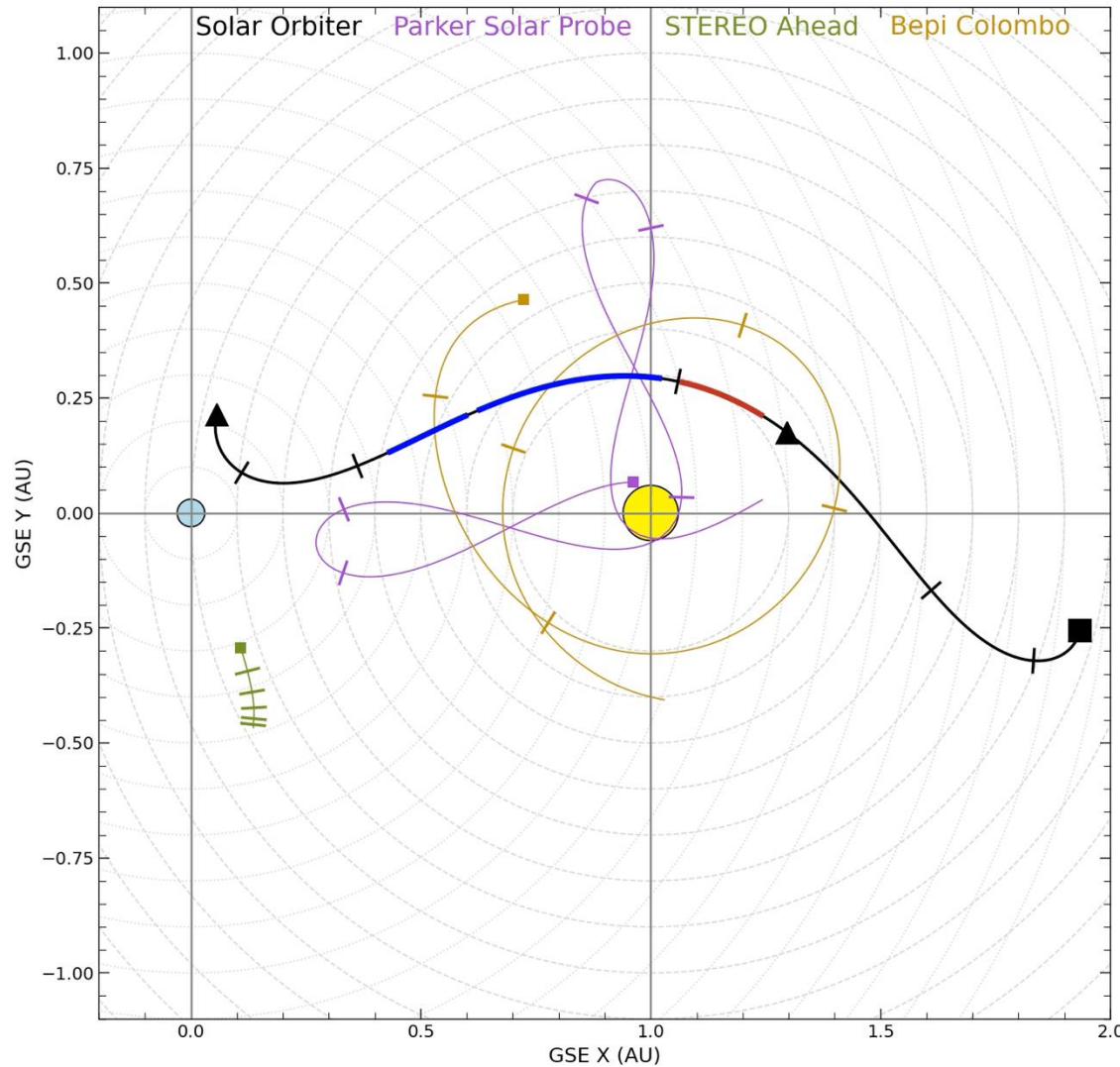


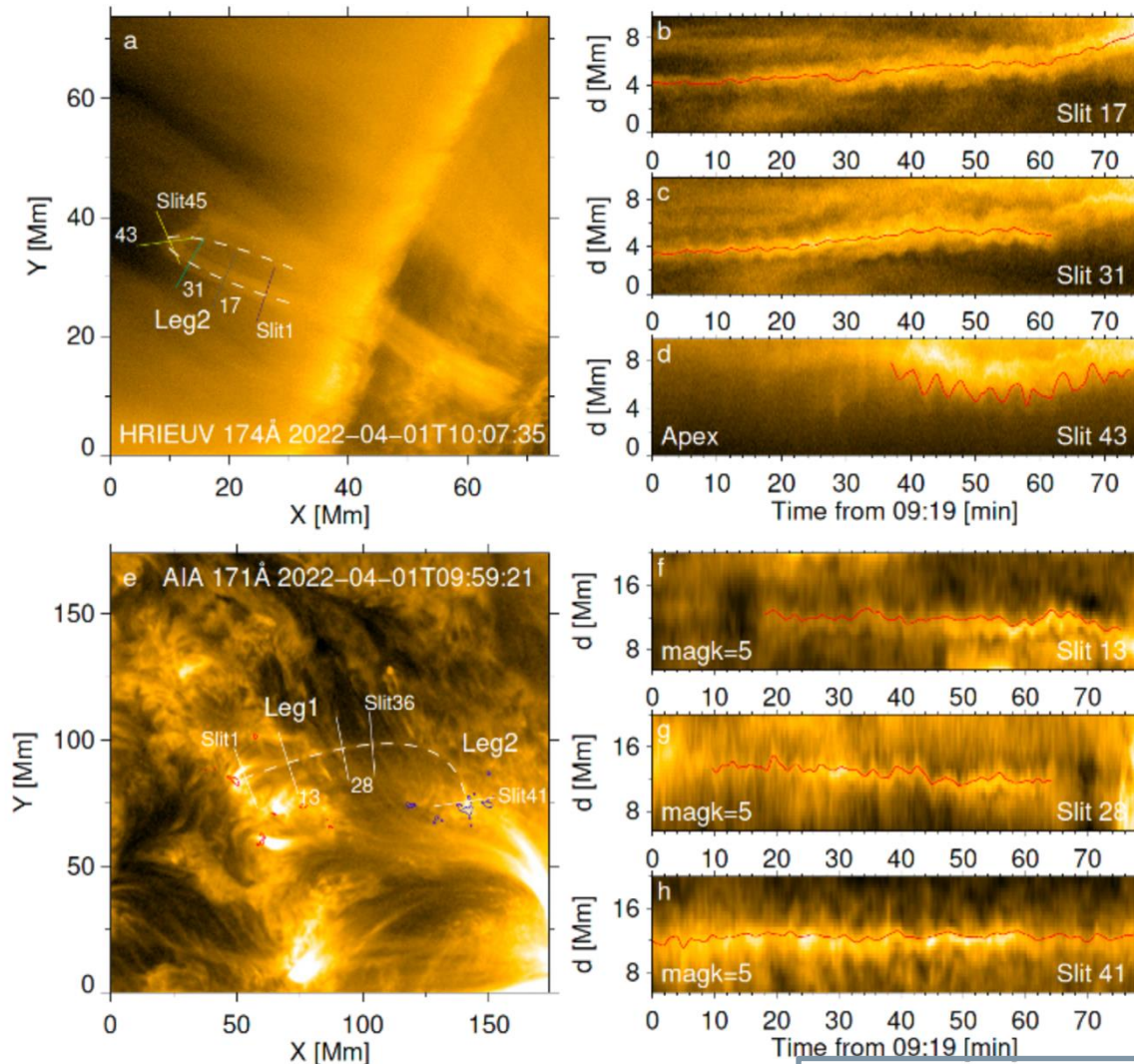
Infer properties (temperature, density, magnetic field) about the background solar atmosphere



Yang et al. (2020)

Multi-Messenger Analyses

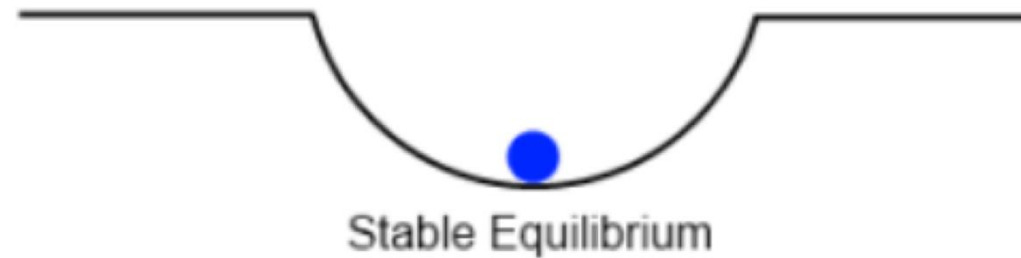




Introduction to MHD Instabilities

What is an instability?

Essentially, an instability is a runaway process that occurs when a magnetic configuration is perturbed from an unstable equilibrium state. MHD instabilities can have many different forms.



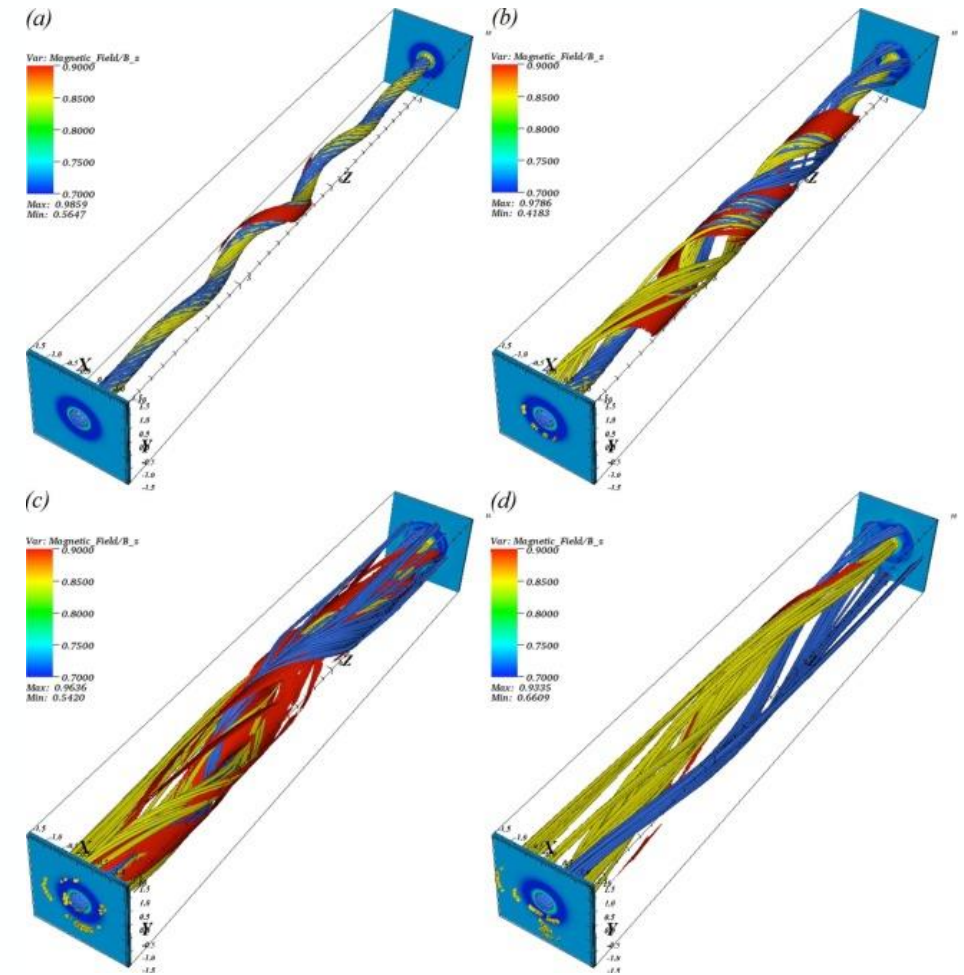
From numerous sources...

There are lots of different MHD instabilities. We certainly don't have time to discuss them all. Some examples are:

- Kink instability
- Torus instability
- Kelvin-Helmholtz instability
- Tearing mode instability
- Bouyancy instability
- Thermal instability
- Rayleigh–Taylor instability

Abstract

We show how some different fundamental plasma processes - the ideal kink instability, magnetic reconnection and magnetohydrodynamic oscillations - can be causally linked. This is shown through reviewing a series of models of energy release in twisted magnetic flux ropes in the solar corona, representing confined solar flares. 3D magnetohydrodynamic simulations demonstrate that fragmented current sheets develop during the nonlinear phase of the ideal kink instability, leading to multiple magnetic reconnections and the release of stored magnetic energy. By coupling these simulations with a test particle code, we can predict the development of populations of non-thermal electrons and ions, as observed in solar flares, and produce synthetic observables for comparison with observations. We also show that magnetic oscillations arise in the reconnecting loop, although there is no oscillatory external driver, and these lead to pulsations in the microwave emission similar to observed flare quasi-periodic pulsations. Oscillations and propagating waves also arise from reconnection when two twisted flux ropes merge, which is modelled utilising 2D magnetohydrodynamic simulations.

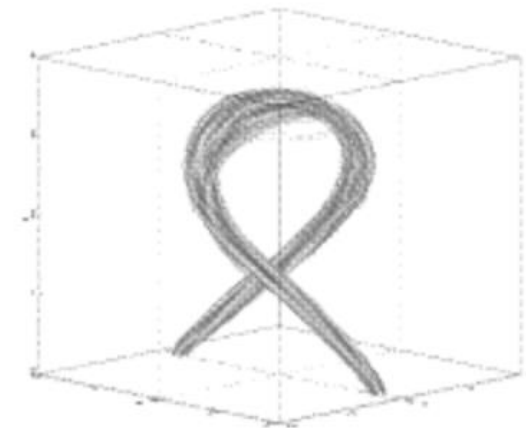
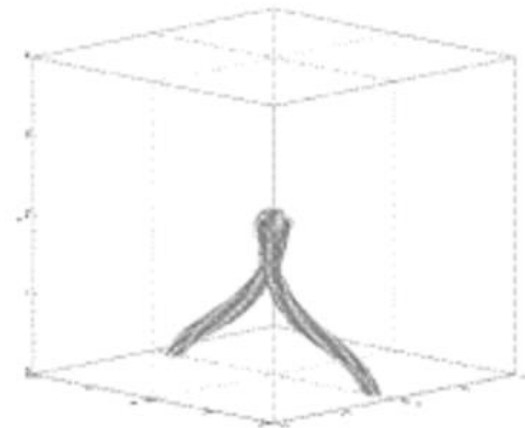
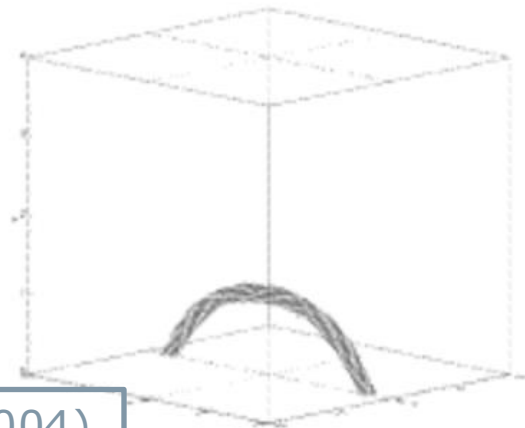
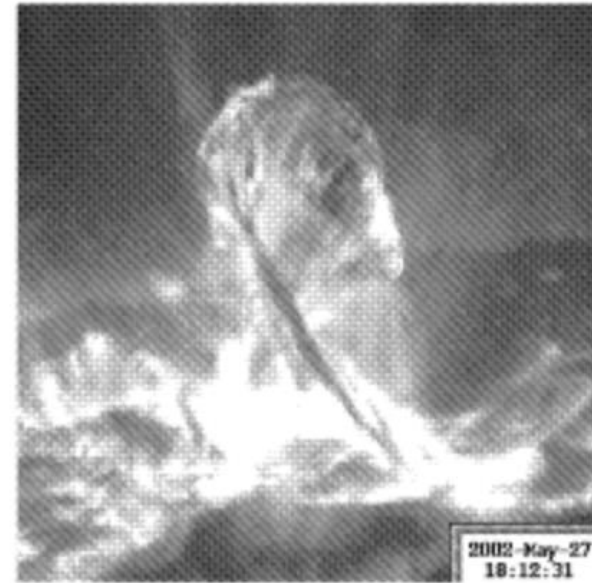
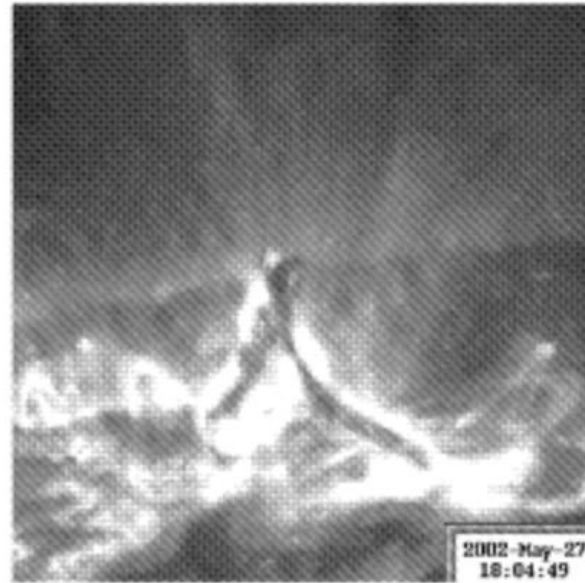
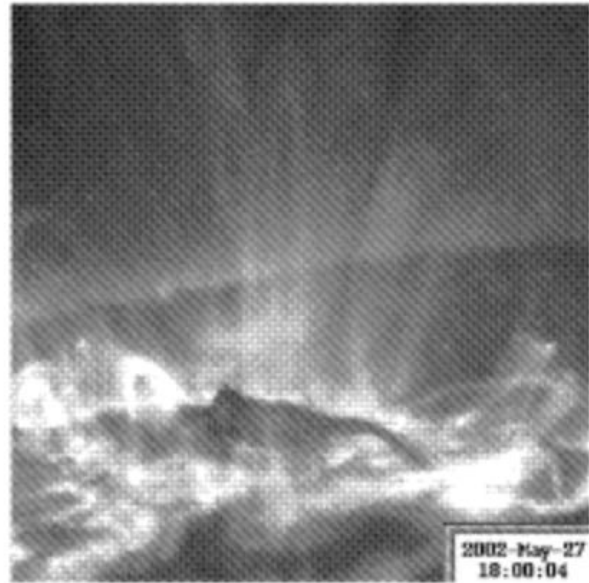


Browning et al. (2024)

Requires twist!

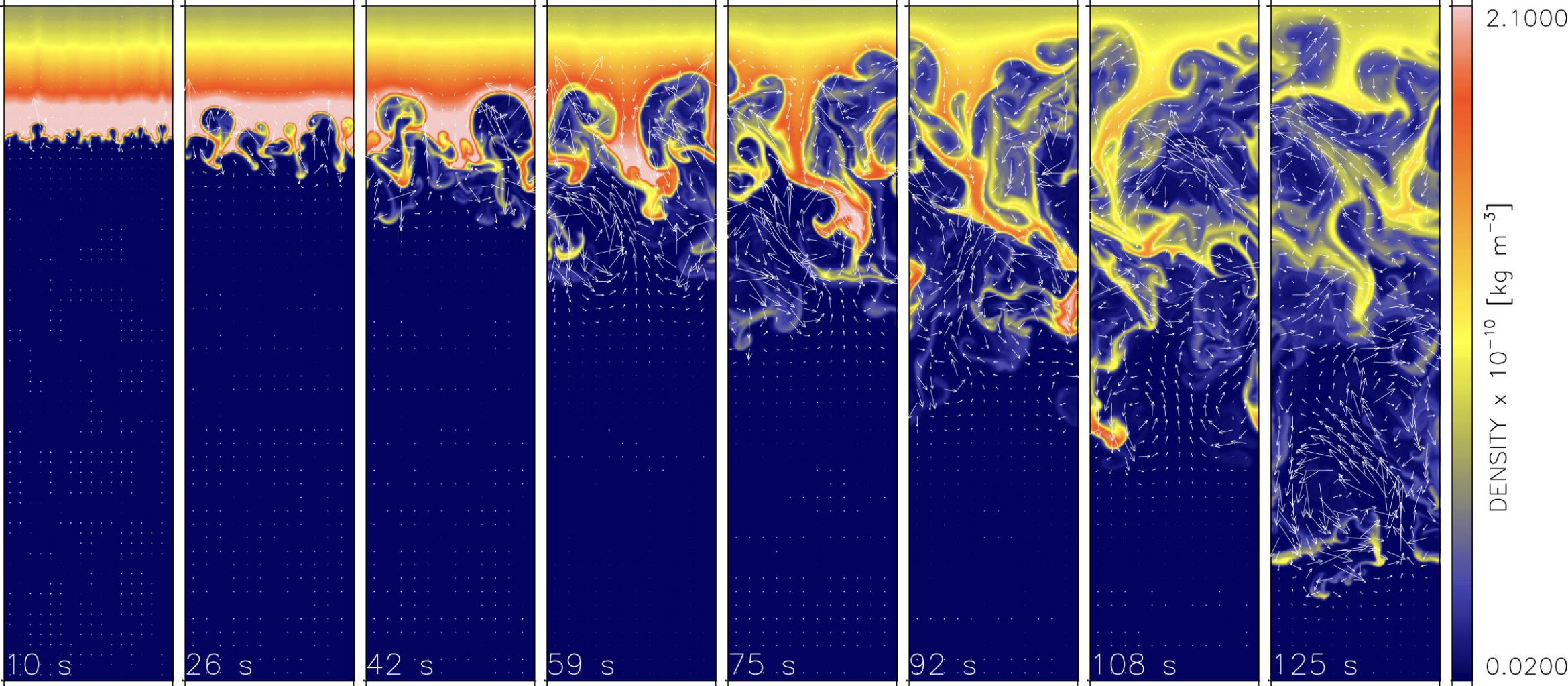
Hood et al. (2009)

Kink instability



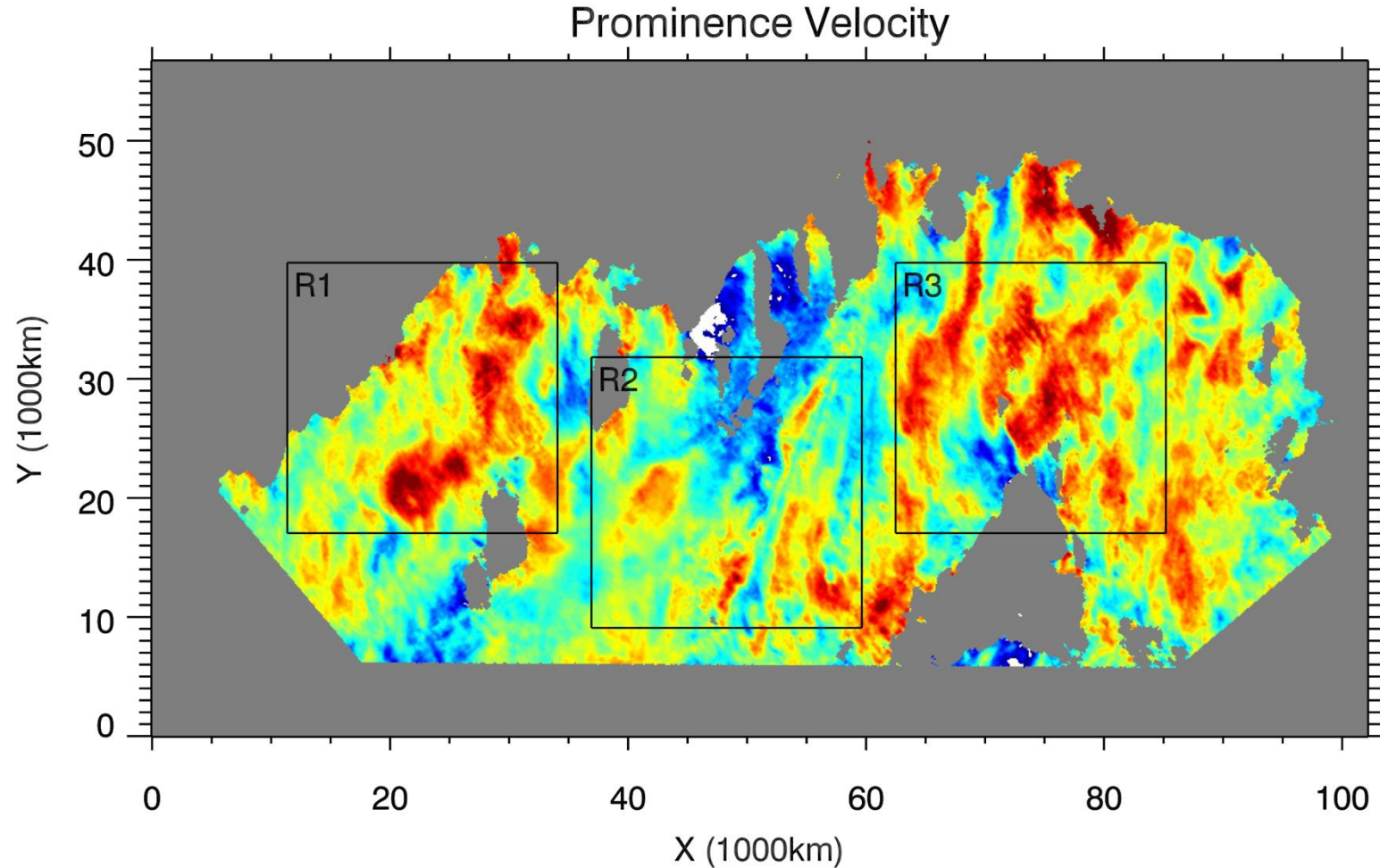
Török & Kleim (2004)

Rayleigh-Taylor instability

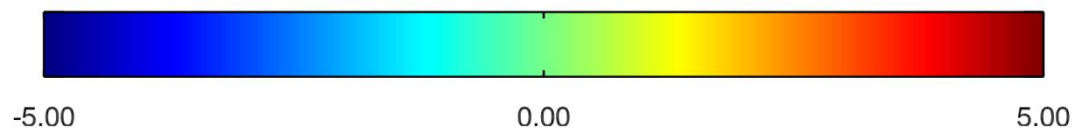


Khomenko et al. (2014)

Rayleigh-Taylor instability

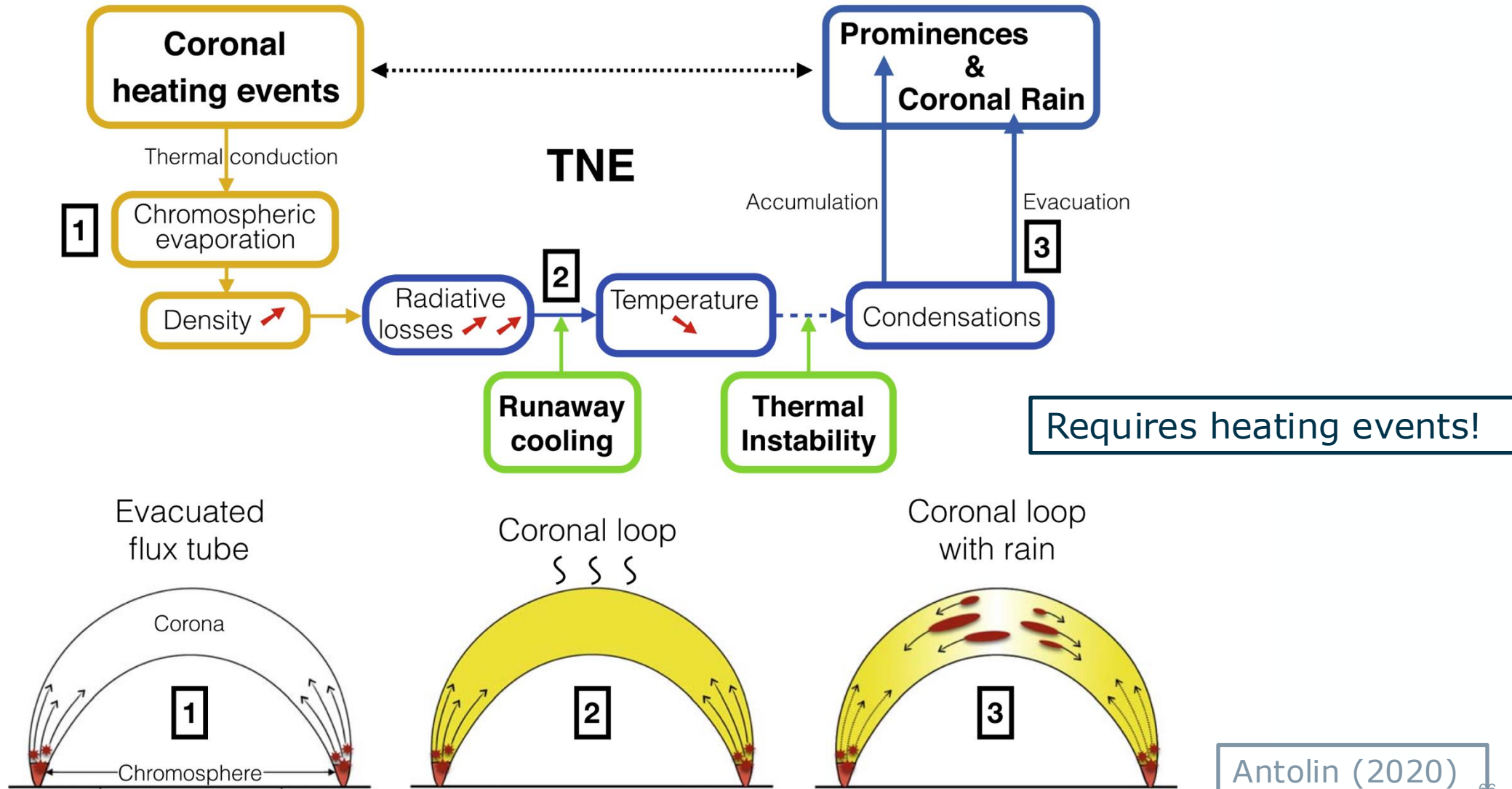


Hillier et al. (2017)

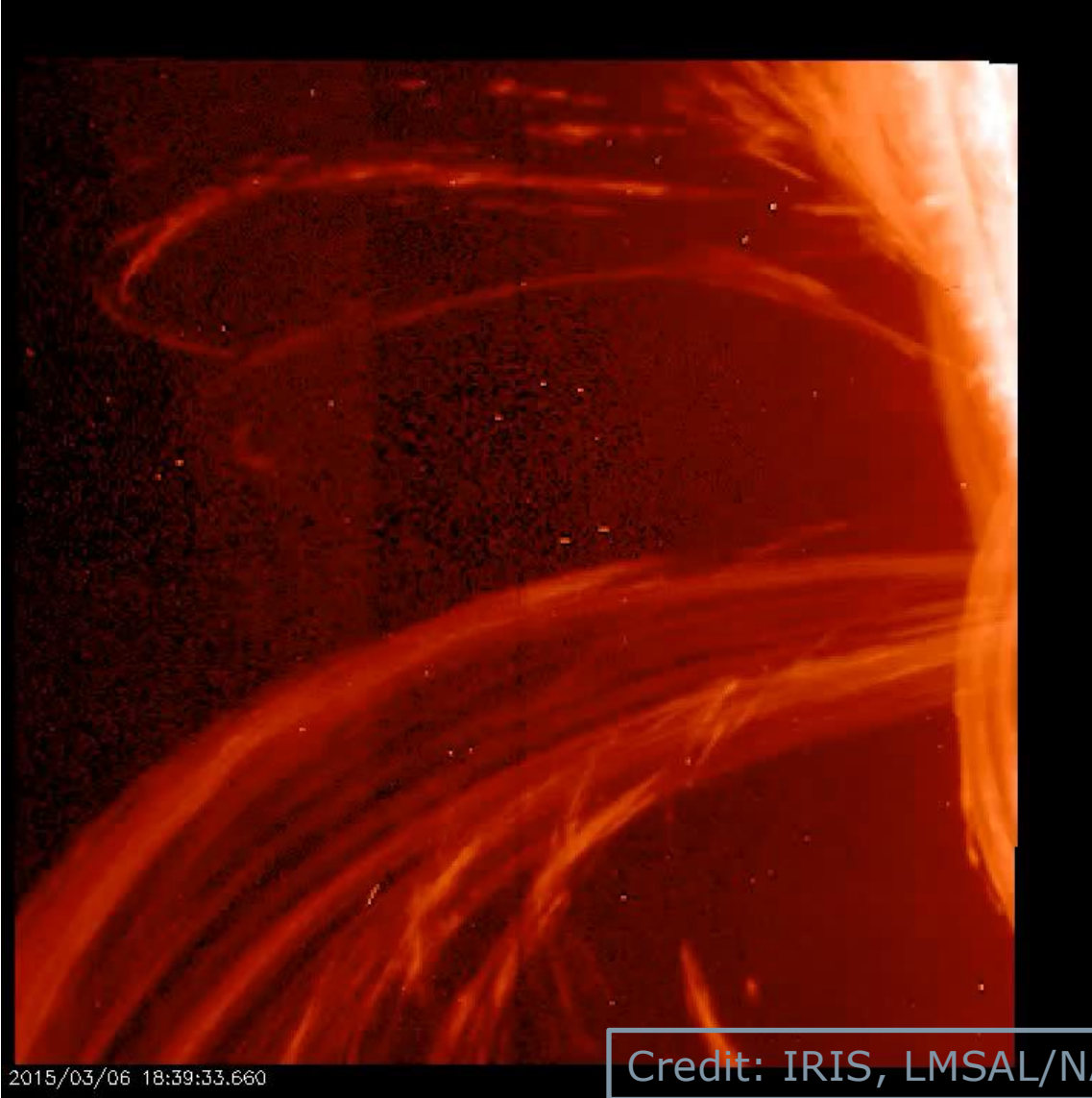


Requires different densities

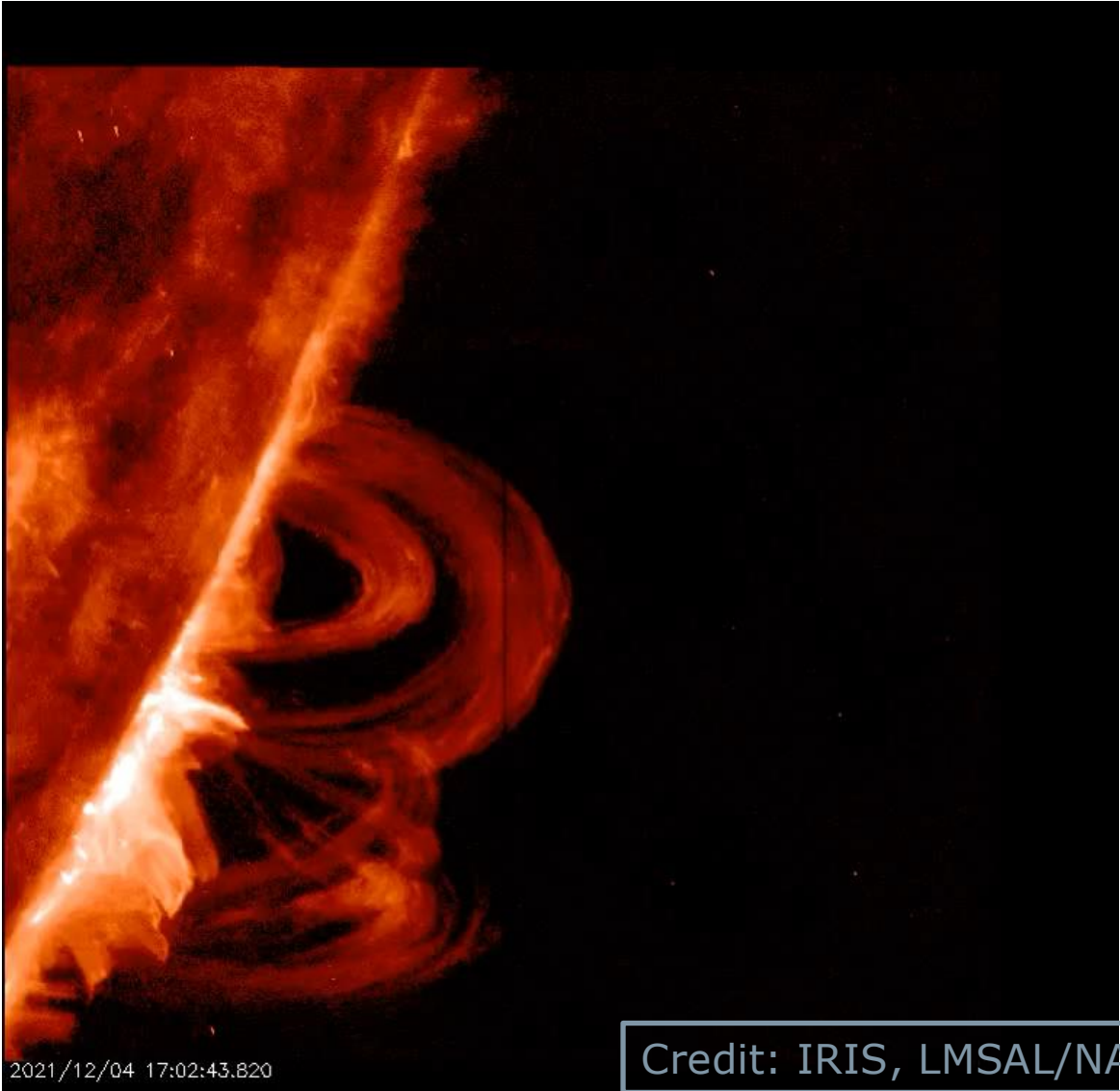
Thermal instability



Thermal instability – Coronal Rain



Thermal instability – Coronal Rain



MHD Waves and Instabilities are everywhere within the solar atmosphere. They could be important for atmospheric heating but also for driving dynamic Space Weather events.

Go out there and investigate them!



What?

- ▶ **independent postdoctoral fellowship for ESA State nationals**
- ▶ research project covering any topic in space science
- ▶ 2 + 1 years (proposal for 3rd year extension)

Where?

- ▶ ESTEC (Netherlands), ESAC (Spain) or STScI (USA)

Why?

- ▶ **100% research time** (optionally <20% functional work, e.g. archive/data science, citizen science, operations, calibration, communication)
- ▶ insights into ESA environment & activities
- ▶ mentoring from senior ESA Science Faculty members
- ▶ training available (e.g. spacecraft design, soft skills, management)
- ▶ 3500-4600€ net monthly salary (depending on location & experience)
- ▶ comprehensive health coverage

ARCHIVAL RESEARCH VISITOR PROGRAMME

To increase the scientific return from its space science missions, ESA welcomes applications from scientists interested in pursuing research based on publicly available data in the [ESA Space Science Archives](#). The [Archives](#) host data from all current and past ESA space science missions in astronomy, planetary science, and heliophysics.

The ESA Archival Research Visitor Programme is open to scientists at all career levels who are affiliated with institutes in [ESA Member States and Collaborating States](#), although we will also consider strong applications from outside those states. Early-career scientists (within 10 years of the PhD) are particularly encouraged to apply, including PhD students ([see below](#)). We encourage applications from women and minorities. The evaluation process is anonymised to ensure equal opportunities for all applicants.

Residence lasts typically between one and three months, also distributed over multiple visits, depending on the complexity of the research project. The research projects can be carried out at [ESAC](#) (Madrid, Spain) and at [ESTEC](#) (Noordwijk, Netherlands). To offset the expenses incurred by visitors, ESA covers travel costs from and to the home institution and provides support for lodging expenses and meals.

During their stay, visiting scientists have the opportunity to interact with archive and mission specialists for questions on the retrieval, calibration, and analysis of archival data. In principle, all areas of space research covered by ESA science missions can be supported. To ensure that technical expertise in the specific area of interest is available at ESAC or ESTEC, applicants should consult the [table of expertise](#) and contact the relevant scientists in their field of interest (this is **very important**). In case of doubts, write to the programme coordinators for assistance at arvp@cosmos.esa.int.